IVYSPRING
INTERNATIONAL PUBLISHER

Theranostics

Research Paper

Interleukin-6 Induced "Acute" Phenotypic Microenvironment Promotes Th1 Anti-Tumor Immunity in Cryo-Thermal Therapy Revealed By Shotgun and Parallel Reaction Monitoring Proteomics

Ting Xue[1], Ping Liu[1], Yong Zhou[2], Kun Liu[1], Li Yang[2], Robert L. Moritz[2✉], Wei Yan[1✉], Lisa X. Xu[1✉]

1. Key Laboratory of Systems Biomedicine (MOE), Shanghai Center for Systems Biomedicine, the School of Biomedical Engineering and MED-X Research Institute, Shanghai Jiao Tong University, Shanghai, China.
2. Institute for Systems Biology, Seattle, WA, USA.

✉ Corresponding author: WY: weiyan@sjtu.edu.cn, Tel: +86-21-34201452; LXX: lisaxu@sjtu.edu.cn, Tel: +86-21-62932302; RLM: robert.moritz@systemsbiology.org, Tel: (206) 732-1244.

Abstract

Cryo-thermal therapy has been emerged as a promising novel therapeutic strategy for advanced breast cancer, triggering higher incidence of tumor regression and enhanced remission of metastasis than routine treatments. To better understand its anti-tumor mechanism, we utilized a spontaneous metastatic mouse model and quantitative proteomics to compare N-glycoproteome changes in 94 serum samples with and without treatment. We quantified 231 highly confident N-glycosylated proteins using iTRAQ shotgun proteomics. Among them, 53 showed significantly discriminated regulatory patterns over the time course, in which the acute phase response emerged as the most enhanced pathway. The anti-tumor feature of the acute response was further investigated using parallel reaction monitoring target proteomics and flow cytometry on 23 of the 53 significant proteins. We found that cryo-thermal therapy reset the tumor chronic inflammation to an "acute" phenotype, with up-regulation of acute phase proteins including IL-6 as a key regulator. The IL-6 mediated "acute" phenotype transformed IL-4 and Treg-promoting ICOSL expression to Th1-promoting IFN-γ and IL-12 production, augmented complement system activation and CD86+MHCII+ dendritic cells maturation and enhanced the proliferation of Th1 memory cells. In addition, we found an increased production of tumor progression and metastatic inhibitory proteins under such "acute" environment, favoring the anti-metastatic effect. Moreover, cryo-thermal on tumors induced the strongest "acute" response compared to cryo/hyperthermia alone or cryo-thermal on healthy tissues, accompanying by the most pronounced anti-tumor immunological effect. In summary, we demonstrated that cryo-thermal therapy induced, IL-6 mediated "acute" microenvironment shifted the tumor chronic microenvironment from Th2 immunosuppressive and pro-tumorigenic to Th1 immunostimulatory and tumoricidal state. Moreover, the magnitude of "acute" and "danger" signals play a key role in determining the efficacy of anti-tumor activity.

Key words: "acute" phase response, cryo-thermal therapy, interleukin-6, parallel reaction monitoring, Th1 anti-tumor immunity.

Introduction

Metastatic breast cancer accounts for the most death for women with an overall 5-year survival rate of approximate 24% [1]. Although current systemic treating approaches such as chemotherapy and target therapy have significantly improved the survival rate of patients, more improvements in therapeutic strategies are desirable towards alleviating the cancer-related symptoms, improving patients' life qualities, as well as extending their survival periods. Recently, thermal therapies including thermal

ablation (> 60°C) and cryosurgery have emerged as intervention strategies and been applied as alternative or adjuvant clinical treatments on metastatic breast cancer, taking advantages of their minimal invasiveness, local targeting and less side effects [2, 3]. The cryo/thermal ablation therapy, a combinatorial variant of the thermal strategies, was reported to generate maximal destruction and larger ablation zones [4, 5], considerable decrease of tumor recurrence [6] and a complete tumor regression rate of 41%, providing a superior approach over thermal ablation or cryosurgery alone [7]. Our group has been working on a novel cryo/thermal system for years [8, 9] and previously reported its application for metastatic breast cancer treatment in animal models. By combinatorial usage of liquid nitrogen and radio frequency, this system incurs a rapid temperature shift between freezing (-20 °C) and heating (50°C) on local primary tumors and thereby delivers a promising therapeutic efficacy with an increased survival rate (60%-70%), free-recurrence and significantly reduced metastasis (70%) [10-12].

Hyperthermia or cryosurgery alone was previously reported to induce tumor cell death via cell membrane destruction, cytotoxicity and coagulative necrosis [13], activating a concomitant immune response [14, 15]. Nevertheless, the biological mechanism has not been comprehensively studied. In the past,, we indicated that cryo-thermal therapy increased the damage region of tumor, and led to severe destruction of tumor blood vessels [8, 16]. Furthermore, we observed an increased local induction of Th1 type cytokines and recruitment of CD4$^+$ and CD8$^+$ T lymphocytes [10, 17], while the accumulation of immunosuppressive lymphocytes were drastically reduced [10, 18]. However, cryo-thermal therapy appears to induce more systematic and profound responses *in vivo*, which therefore appeals for a comprehensive and system-wide analysis towards better understanding the anti-tumor mechanism at a molecular level.

Mass spectrometry based proteomics provides such a powerful tool to systematically study protein proprieties and profiles in a complex biological system [19]. To date, high throughput proteomics involves two main strategies. The first is referred as "shotgun" or "discovery" proteomics characterized by data-dependent acquisition (DDA) on mass spectrometer, allowing detection of thousands of proteins per analysis. The other is called "target" proteomics, which permits reproducible quantification of targeted proteins in large scale samples (*e.g.* clinical samples). Among the target proteomics approaches, selected reaction monitoring (SRM) is the first generation and stands as the golden standard so far, which was successfully applied in clinical biomarker discovery [20]. Recently, a new targeted method, called parallel reaction monitoring (PRM), operated in the high resolution and high mass accuracy spectrometers (*e.g.* Q-Exactive) provides an alternative to SRM [21, 22]. Different from SRM, in which fragments per peptide (termed as transitions) are monitored once at a time, PRM allows simultaneous monitoring of all transitions as a full MS/MS scanning profile and thus provides an enhanced selectivity and confidence in quantitation of each analyzed target protein [23].

As a primary component of circulatory system, serum is the major reservoir of thousands of proteins secreted or "leaked" from a broad spectrum of cells and tissues. Proteome changes in serum well reflect the host response to physiological and pathological perturbation. Therefore, serum is regarded as a good window for systematic investigation of the therapeutic responses using proteomics. However, the extreme complexity and huge dynamic range (over 10 orders of magnitude) of serum significantly restricted its application in proteomics via mass spectrometry [24]. Recently, specific focus on N-linked serum glycoproteins has been demonstrated as an effective way to reduce serum complexity, maximize the detective dynamic range and improve the efficiency of low abundant proteins measurement [25]. Moreover, numerous evidences support that alteration in glycoprotein abundance and glycan composition are closely associated with aberrant physiological state, such as cancer and other infectious diseases [26-28].

In this study, we applied cryo-thermal therapy on a highly malignant murine 4T1 breast cancer xenograft model. Serum samples underwent therapy or in control were comprehensively analyzed by shotgun proteomics following N-glycopeptides enrichment, iTRAQ-labeling, and off-gel fractionation. Subsequently 23 glycoproteins were further selected for validation using PRM technique in a total of 94 enriched serum samples over 8 time points. We found that cryo-thermal therapy reshaped the tumor chronic inflammatory microenvironment to an "acute" phenotype, which played a key role to hamper immunosuppression and recover the host anti-tumor immunity. Moreover, the magnitude of "acute" and "danger" signals could determine the efficacy of anti-tumor immunity. The study allowed us to dissect the network of protein changes associated with the cryo-thermal therapeutic efficacy, thus deepening our understanding of its mechanism at the molecular level, and providing insights and guidance to improve this cancer treatment with better therapeutic effects.

Experimental Procedures

Animal experiments

Cell culture

4T1 mouse mammary tumor cell line was obtained from Shanghai First People's Hospital (Shanghai, China). Cells were maintained in Dulbecco's Modified Eagle's Medium (DMEM; GE Healthcare, Logan, UT) supplemented with 10% fetal bovine serum (FBS, Gemini Bio-Products, West Sacramento, CA), 100 units/ mL penicillin and 100 µg/mL streptomycin at 37 °C in a humidified 5% CO_2 incubator.

Xenograft breast tumor model and cryo-thermal / cryo- / hyperthermia therapy

Pathogen-free female Balb/c mice (4 weeks old) were obtained from Shanghai SLAC Laboratory Animal Co., Ltd., and housed at constant temperature and humidity with a 12-h light cycle. All animals were allowed food and water *ad libitum* until ~20 *g* before experiments (approximately 6-week old). All animal experiments were approved by the Animal Welfare Committee of Shanghai Jiao Tong University.

Tumor was induced by injection of $5×10^5$ 4T1 cells subcutaneously into the right dorsal region of mouse and received cryo-thermal therapy 3 weeks later, reaching the size of ~10 mm in diameter. Cryo-thermal therapy was performed using a modified protocol [11]. Briefly, a thermocouple was inserted to the bottom of tumor to monitor the local temperature in real time. Firstly, tumor was rapidly frozen to -20 °C by liquid nitrogen and maintained for 5 min. Subsequently, liquid nitrogen was turned off and frozen tumor was recovered naturally to 8 °C. Finally, radiofrequency (460 kHz) was introduced to heat the tumor (10 min, 50 °C). Afterwards, mice under cryo-thermal or no treatment as controls were kept for survival rate observation. Tumor volume was monitored and measured by the length (L), width (W) and height (H), and calculated as V=π/6×L×W×H. Lungs were harvested and fixed in Bouin's solution (Sigma-Aldrich, St. Louis, MO). For time course proteome analysis, another group of mice were kept for another 2 h, 2, 5, 8, 11, 14, 21 and 28 days post therapy, respectively and mice left untreated were taken as control with matching time points. In addition, 8-week-old healthy mice were taken as "healthy group". Plasma from each mouse was taken for proteomic analysis.

For cryotherapy, tumor was rapidly frozen to -20 °C by liquid nitrogen and maintained for 15 min. For hyperthermia therapy, radiofrequency (460 kHz) was introduced to heat tumor (15 min, 50 °C). Sera were collected 2 days post therapy.

Sample preparation for proteomics analysis

Serum N-glycosylated peptides capture

Plasma was left to be clotted (30 min, 25°C) and centrifuged (500 *g*, 10 min, 4 °C) and the supernatant (serum) was collected. Prior to glycopeptide capture, serum in each condition (n=5~8) was pooled to minimize the individual variance. Serum concentration was determined using BCA assay (Thermo Fisher Scientific, San Jose, CA).

Subsequently, 25 µL of each pooled sample was processed and subjected to glycopeptide capture. Briefly, samples were first diluted to 100 µL with 0.1 M NH_4CO_3, and denatured with 50% TFE (Trifluoroethanol)/0.1% SDS (30 min, 55 °C). Samples were reduced with 8 mM TCEP (30 min, 55 °C) and alkylated with 12 mM iodoacetamide (30 min, 25 °C) in the dark (all of the reagents were obtained from Sigma-Aldrich, St. Louis, MO). Samples were then diluted with 0.1 M NH_4CO_3 to a final concentration of 5% TFE and digested overnight at 37 °C with sequencing grade modified trypsin (1/50, w/w; Sigma-Aldrich, St. Louis, MO). After digestion, samples were acidified with 1% formic acid to quench the reaction and desalted on C18 reverse-phase spin columns according to the manufacturer's instructions (100 mg, Waters, Milford, MA), dried under vacuum to ~ 100 µL before glycopeptide capture.

N-glycopeptide capture procedure was carried out according to a published protocol [25] with a slight modification. Briefly, desalted peptides were treated with 10 mM sodium periodate (30min, 25°C ,dark) to oxidize the cis-diol groups on glycans. The oxidized glycopeptides were then coupled to hydrazide resin (Bio-Rad, Hercules, CA) by the reaction of aldehyde groups. The extensively washes were performed to remove non-glycosylated peptides with three times of 1 mL of 8M urea/0.1% SDS, 1.5 M NaCl, 80% ACN, Milli-Q H_2O and 50mM NH_4CO_3. N-glycopeptides were then released by PNGase F (New England Biolab, Ipswich, MA).

iTRAQ labeling and off-gel electrophoresis

iTRAQ labeling was carried out using iTRAQ reagent 8-plex kit (Sciex, Framingham, MA) according to the manufacturer's introduction. Cleaved N-glycopeptides were desalted, dried and labeled with different isobaric tags (2 h, 25°C) and quenched by Milli-Q water. Labeled peptides from multiple time points were assigned to three groups and mixed (Additional File 7: Figure S2C). N-glycopeptides enriched from healthy sera (n=8) were labeled with 119 tag and evenly assigned to three groups as global reference (Additional File 7: Figure S2C). Formally N-glycopeptide mixtures were separated by OFFGEL

fractionation (24 wells, 3-10 pI strips) in a 3100 OFFGEL fractionator (Agilent Technologies, Santa Clara, CA) according to the manufacture's instructions. Afterwards, peptide mixtures were collected from each well and pooled into 8 different fractions (A: 1-3; B:4-6; C:7-9; D:10-12; E:13-15; F:16-18; G: 19-21; H: 22-24). Fractions were desalted on C18 columns (50 mg, Waters, Milford, MA), dried under vacuum and dissolved in 0.1% formic acid prior to data-dependent LC-MS/MS analysis.

LC-MS/MS acquisition

Shotgun data-dependent acquisition (DDA) MS

Approximately 0.5 μg of glycopeptides from each fraction were separated in a 2-h gradient on a 15-cm long (75 μm inner diameter) PicoFrit Self-Pack Column (360 μm OD, 75 μm ID, 15 μm Tip, New Objective, Woburn, MA) packed in-house with 3 μm 200 Å C18 particles (Dr. Maisch GmbH). Reverse phase chromatography was performed with an EASY-nLC 1000 ultra-high-pressure system, which was coupled to an Orbitrap Elite mass spectrometer interfaced with a nanoelectrospray ion source (Thermo Fisher Scientific, San Jose, CA). Peptides were loaded to a trap column (150 μm× 12 mm) at 10 μL/min with solvent A (0.1% (v/v) formic acid) and eluted with a linear 120-min gradient of 2% to 35% solvent B (0. 1% (v/v) formic acid, acetonitrile) at a flow rate of 300 nL/min. After each gradient, the column was flushed with 80% solvent B for 10 min and equilibrated with 2% buffer B for another 20 min. MS data were acquired with a shotgun proteomics method, where in each cycle, a full scan was acquired at a resolution of 30,000 at *m/z* 400 with a mass range of 380-1600 *m/z*. Up to 15 most intense precursor ions with charge ≥ 2 were selected with an isolation window of 2 Da and subsequently fragmented by higher-energy collisional dissociation (HCD) with normalized collision energy of 40%. The MS/MS scans were acquired at a resolution of 15000 at m/z 400 with fixed first mass of 100 Da. The precursor ions were dynamically excluded from reselection for 60 s, and the exclusion list size was 500. Peptides in each fraction were analyzed for two technical replicates. Additionally, to evaluate the efficiency of N-glycopeptide capture, prior to the iTRAQ labeling and fractionation, glycopeptides extracted from each pooled sera were analyzed on the Orbitrap Elite mass spectrometer, respectively.

Target analysis by Parallel reaction monitoring (PRM)

The targeted quantification and verification were carried out in 94 serum samples with 5~6 mice in each condition without pooling, across 8 time points. 23 proteins were selected with 1~4 peptides, resulting in 33 precursors in total (Additional File 1: Table S1). Glycopeptides were enriched as above and one of the angiotensin peptides was spiked in as the standard reference. PRM analysis was performed by Q-Exactive Plus mass spectrometer (Thermo Fisher Scientific, San Jose, CA) with the same 2 h LC gradient setting as above. The MS acquisition mode was a combination of two scan events: a full scan and a time-scheduled scan. The full scan was taken at a resolution of 70000 at m/z 200 with a scan mass range of 200 to 1800 m/z, a target (AGC) of 1e6 and maximum injection fill time is 200 ms. The scheduled scan was employed at a resolution of 35000 at m/z 200, a target AGC of 5e5, and maximum injection fill time is 105 ms. The precursor ion of each target peptide was isolated with 2 Da window. The elution time window was set as +/- 5 min. Precursor ions were fragmented with normalized collision energy of 27%. The complete data acquisition took 15 days of mass spectrometer time.

Computational MS data analysis

Shotgun data dependent MS

MS raw files from DDA acquisition were analyzed by the Trans-Proteomic Pipeline software suite (TPP, Institute for Systems Biology, Seattle, WA) (version 4.7.0). Raw files were first converted to centroid mzXML and MS/MS spectra acquired were searched with comet (version 2.0) against a combined UniProtKB/Swiss-Prot and UniProtKB/VarSplic mouse database downloaded [29] with reversed sequences. Common contaminants [30] were included. Searching parameters were used as follows: precursor ion mass tolerance: ±10 ppm; fragment ion mass tolerance: 0.02 Da; semi-tryptic termini and two missing cleavages were allowed; fixed modification: carbamidomethylation (C); isobaric modification of lysine and peptide N-terminal residue; dynamic modification: oxidation (M) and deamidation (N). Searching results were further processed with PeptideProphet and ProteinProphet embedded in TPP. False discovery rate (FDR) for protein was set to 0.01. Isobaric labeling quantification was performed by LIBRA integrated in TPP and only unique N-glycopeptides with a PeptideProphet score ≥ 0.85, corresponding to an FDR <0.01 were considered for N-glycosylated protein quantification. The efficiency of glycopeptide capture was carried out and measured as the percentage of peptides with NXS/T sequence motif (X represents any amino acid residue except proline) in total peptides and corresponding glycosites were checked in Uniprot manually. The shotgun mass spectrometry proteomics data have been deposited to the ProteomeXchange Consortium [31] via the PRIDE partner repository with the dataset

identifier PXD003136.

PRM MS analysis

MS raw data acquired from target proteomics analysis was searched with SEQUEST integrated in Proteome Discover (version 1.4, Thermo Fisher Scientific, San Jose, CA) against the same database and search parameters described above. Peptide probabilities were calculated by the Percolator algorithm in Proteome Discover and false discovery rate was set to 0.01. The generated .msf file was used to create a library in Skyline (version 3.1.0) [32] and the cut-off score was set as 0.90. The target precursors list was then uploaded to Skyline and the 6 most intense product ions matching the library were selected as transitions. Peak picking was manually checked and corrected according to the transitions, retention time, mass accuracy and MS/MS spectra. The area under curve (AUC) of each transition was extracted and exported to Excel for further data analysis.

Bioinformatics analysis and statistics

Shotgun MS data normalization

For shotgun MS data, the intensities of reporter ions were used as a proxy of protein abundances. Each protein's abundance was divided by its channel's global reference and the median value was obtained and centered to 1 to equalize the intensities between runs [33]. After normalization, we assessed the correlation of technical replicates for each sample, which well fit a line with an average R^2 of 0.875 (Additional File 2: Table S2). In this case, protein's abundances from two technical replicates were acquired and averaged to improve the quantification accuracy.

For PRM MS data, each sample's average base peak intensity was extracted from the full scan acquisition using RawMeat (version 2.1, VAST Scientific, www.vastscientific.com). The normalization factor for sample N was calculated as f_N= the average base peak intensity of sample N/the median of average base peak intensities of all samples. The AUC of each transition from sample N was multiplied by this factor. After normalization, the AUC of each transition was summed to obtain AUCs at the peptide level. Relative protein's abundance was defined as the intensity of a certain peptide.

Statistical analysis

Unsupervised hierarchical clustering analysis was handled in R package with default parameters for distance and similarity calculation. Ingenuity Pathway Analysis platform (IPA, QIAGEN Redwood City, www.qiagen.com/ingenuity) was used to analysis the enriched pathways and functional annotation. Other statistical analysis was performed in GraphPad prism 5 (version 5.01, San Diego, CA). Data were presented as the mean ± standard deviation (SD). A two-sample, two-side student t-test was applied to compare the difference between the mean values of two groups. Two-way ANOVA was used for multiple groups' comparison with Bonferroni post-test.

Enzyme-linked immunosorbent assay (ELISA) for interleukin-6 (IL-6) assessment

IL-6 level in serum was measured by ELISA using commercial kits (R&D Systems, Minneapolis, MN) according to the manufacturer's instructions. Serum samples were collected 2, 24, 48 and 264 h after treatment. Triple biological and two technical replicates were performed. Expression level was compared to that of mice untreated.

Neutralization of IL-6 *in vivo*

Mice injected with 4T1 cells were treated as described above. 100 μg of mouse anti-IL-6 Ab or control rat IgG Ab (Sanjian, Tianjin, China) was intraperitoneally injected to mice 3 and 24 h post cryo-thermal therapy. Mice were sacrificed 2 days post therapy and serum was collected.

Western blot analysis of acute phase proteins

Sera from different therapeutics (cryo-thermal /cryotherapy/hyperthermia/no treatment) and IL-6 neutralization were collected 2 days post therapy and subjected to 12% SDS-PAGE gel. Protein amount was evaluated with Ponceau S (Beyotime, Shanghai, China). Target proteins were immunoblotted with specific Abs as following: anti-APCS, anti-ORM1 (1:500, Absci, Baltimore, MD) and anti-HP (1:500, Proteintech, Rosemont, IL). Each protein was analyzed on three independent mice with three technical replicates. Blots were evaluated with Quantity One 1-D (Bio-Rad, Hercules, CA). Results are expressed as relative pixel intensity normalized with control group.

Quantitative reverse transcription–PCR

Real time PCR was applied to examine the level of IL-6 within primary tumors and IL-12, IFN-γ within spleens. 24 h or 3 days after therapy, primary tumors or spleens were harvested and homogenized with gentle MACS Dissociator (Miltenyi Biotec Technology, Bergisch Gladbach, Germany). RNA was extracted in Trizol (Invitrogen™, Thermo Fisher Scientific, San Jose, CA) reagent and reverse transcribed to cDNA using Superscript III (Invitrogen, Thermo Fisher Scientific, San Jose, CA) according to the manufacturer's instructions. β-actin was used as

the control transcript. Primer sequences used were as follows:

IL-6-FW5'-GACAAAGCCAGAGTCCTTCAGAGAG ATACAG-3';
IL-6-RV5'-TTGGATGGTCTTGGTCCTTAGCCAC-3';
IL-12p40-FW5'-TGGTTTGCCATCGTTTTGCTG;
IL-12p40-RV5'-ACAGGTGAGGTTCACTGTTTCT;
IFN-γ-FW5'-CCATCCTTTTGCCAGTTCCTC;
IFN-γ-RV5'-ATGAACGCTACACACTGCATC;
β-actin-FW5'-CATGTACGTTGCTATCCAGGC-3';
β-actin-RV5'-CTCCTTAATGTCACGCACGAT-3'.

Difference in expression of IL-6, IL-12 and IFN-γ compared to mice untreated was determined by calculating the fold change in expression (2^{-ddCT}).

Flow cytometry

Spleens were extracted after therapy and mechanically homogenized with gentle MACS Dissociator to obtain a single-cell splenocyte suspension. Erythrocytes were removed with 1× red blood lysis buffer (1.5 mM NH_4Cl, 120 mM $NaHCO_3$, 1 mM Na_2-EDTA). Single-cell suspensions were stained with the following Abs: FITC-anti-mouse-CD3, PE-anti-mouse-CD4, APC-anti-mouse-CD8, PerCP-Cy5.5-anti-mouse-CD26, Alex fluor 488-anti-mouse-CD11c, PerCP-Cy5.5-anti-mouse-MHCII, PE-anti-mouse-CD86, PE-anti-mouse-Gr1 and FITC-anti-mouse-CD11b. Abs were obtained from eBioscience (San Diego,CA) and BioLegend (San Diego, CA). Samples were measured with FACSAria II (BD Biosciences, Mountain View, CA) and analyzed using FlowJo analysis software (Tree Star, Ashland, OR).

Results

Cryo-thermal therapy significantly improved cancer survival rate and reduced metastasis

In present study, we applied cryo-thermal therapy on spontaneous metastasis murine breast cancer xenograft model to examine its efficacy (Figure 1A; Materials and Methods). 21 days post tumor inoculation, metastases started to be observed in lungs (Figure 1D).
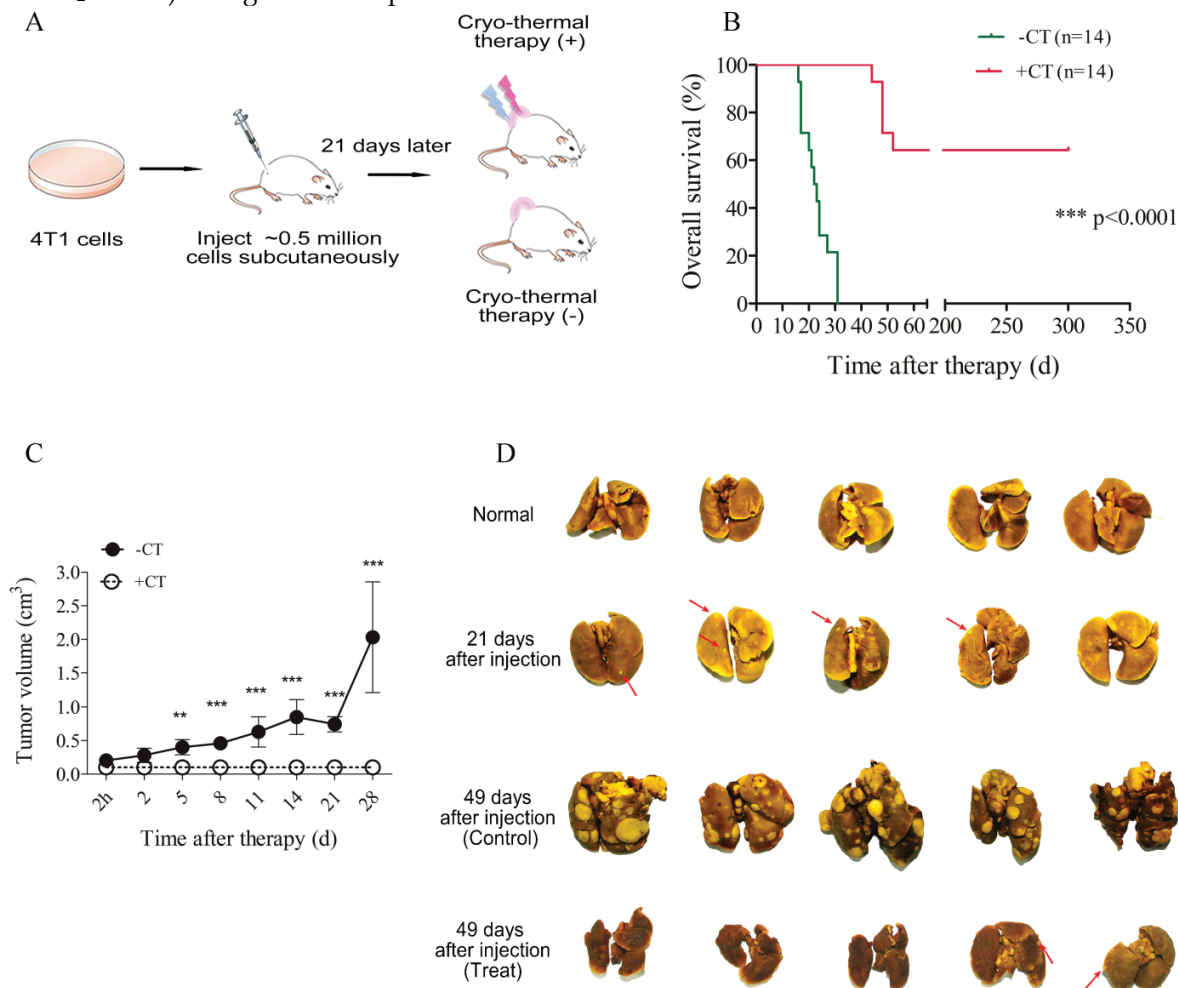

Figure 1. The schematic graph of cryo-thermal therapy using murine breast tumor model and the therapeutic efficacy. (A) Balb/c female mice were s.c. injected with 5×10⁵ 4T1 cells and received treatment after 3 weeks. (B) Kaplan-Meier survival curve. Survival curves were compared using log-rank tests. ***p<0.0001. (C) Tumor growth curves. (D) Cryo-thermal therapy could effectively inhibit or reduce tumor metastasis to lung. Data are shown as mean ± SD. **p < 0.01, ***p < 0.001 by two-way ANOVA with the Bonferroni correction. n=14 per group.

In this situation, 14 mice underwent cryo-thermal therapy and 14 without treatment as the control. Healthy mice were taken as "normal" group. In mice treated, significantly prolonged survival rate (64%) was achieved, however, all of the untreated mice died within 50 days after tumor inoculation (Figure 1B). Tumor growth concomitant with high mortality was observed in untreated group, indicating its poor prognosis, whereas in therapeutic group, tumor shrank immediately after therapy, scared over time and consequently healed without tumor recurrence (Figure 1C, Additional File 7: Figure S1). Moreover, dramatic increase of metastasis was observed in control mice accompanied by severe lung swelling. By contrast, metastasis was extensively limited or undetectable after therapy, and meanwhile lung's volume was similar to that of healthy mice (Figure 1D). Taken together, these results suggested that local cryo-thermal therapy provided a promising strategy to hamper primary tumor progression, eradicate or attenuate the development of distant metastasis, and therefore contributed to a good outcome of survival.

Shotgun proteomics identification and quantification of serum glycosylated proteins

To comprehensively investigate the underlying tumor suppression mechanisms by cryo-thermal therapy, a time course study over 8 time points was carried out to compare the serum proteome changes between post- and non-treatment mice (Figure 2). Serum samples under each condition (n=5~8) were pooled and analyzed using iTRAQ-based quantitative proteomics technology focusing on N-linked glycoproteome [25]. By applying the hydrazide chemistry to specifically enrich N-glycosylated proteins, more than 90% of the identified peptides, corresponding to 96% glycoproteins under each condition contained the N-glycosylation signature of NXS/T motif, suggesting a high specificity of the enrichment in serum samples (Additional File 7: Figure S2A and B). In total, we identified 3002 unique peptides corresponding to 308 proteins at a false discovery rate (FDR) of 1% (Figure 3A left panel, Additional File 7: Figure S2D left panel, Additional File 3: Table S3). By projecting these identified proteins into the published Peptide-Atlas database [34], we found that their detectable dynamic range was largely enhanced (7 vs 4 orders of magnitude in crude plasma[35]), with the minimal detection level of ng/mL (Figure 3B). Of the identified proteins, 241 were annotated as N-glycoproteins, 231 of which were quantified (Figure 3A right panel, Figure S2D right panel, Additional File 4: Table S4). We analyzed the subcellular localization of the 231 quantified proteins

and there were 118 (51%) and 59 (26%) proteins categorized as "extracellular" and "plasma membrane" respectively (Additional File 7: Figure S3A), which fit well with the properties of glycoproteins and is consistent with the composition of serum system. To better profile the proteome change in response to cryo-thermal therapy, protein ratios between treated and untreated mice were calculated and transformed to the logarithm scale which fitted a normal distribution (Figure S3B). Proteins with ratios outside the range of mean ± 2σ at one or more time points were considered as significant proteins in the following data mining. Overall, a total of 53 significant glycoproteins were determined across the entire time course, and 11 on average were obtained for each time point (Additional File 5: Table S5)

Acute phase response was the most enriched pathway in response to cryo-thermal therapy

After obtaining 53 proteins significantly changed during the time course, we first performed an enriched pathways analysis using Ingenuity Pathway Analysis (IPA) software to reveal the significantly affected canonical pathways. Acute phase response (p value = 3.64E-06) was the most enriched pathway. Interestingly, all of the significant proteins were elevated on the 2nd day post therapy (Additional File 7: Figure S4A). However, such up-regulated expression turned to be down-regulated (Figure S4B) on the last two days.

Quantitative time course measurement of induced proteome changes

Next, to get a better visualization of a global proteome change over the time course, we performed an unsupervised hierarchical clustering according to the logarithm ratios on 34 significant proteins with no missing values. As shown in Figure 4A, hierarchical clustering distinguished the proteome to early and late response, in which before day 2, they appeared to be similar in expression patterns, however, at the other six time points, they showed a markedly distinct profile. Such differential expression revealed that the overall response to cryo-thermal therapy was time-characterized. In addition, proteins were hierarchically clustered into 4 groups, annotated with different biological functions. Besides the 'acute phase response' in cluster 'c', proteins contained in cluster 'a' were mostly up-regulated during the late time points. They are broadly associated with tumor progression. Proteins grouped in cluster "b" are mostly involved in carbohydrate and lipid metabolism. These proteins were commonly unchanged in the early time periods while elevated on

the 28th day. Proteins clustered in 'd' were partially associated with leukocyte movement, and they are mostly down-regulated during the late stage.

Overall, the integrated analysis of pathway and supervised clustering revealed that cryo-thermal therapy induced diverse biological responses and they were time-dependent. In terms of the timeframe, acute phase response was the first-end event, encompassing all of the biological responses. These findings implied that acute phase response played an important role in modulating tumor progression and carbohydrate/lipid metabolism (Figure 4B).
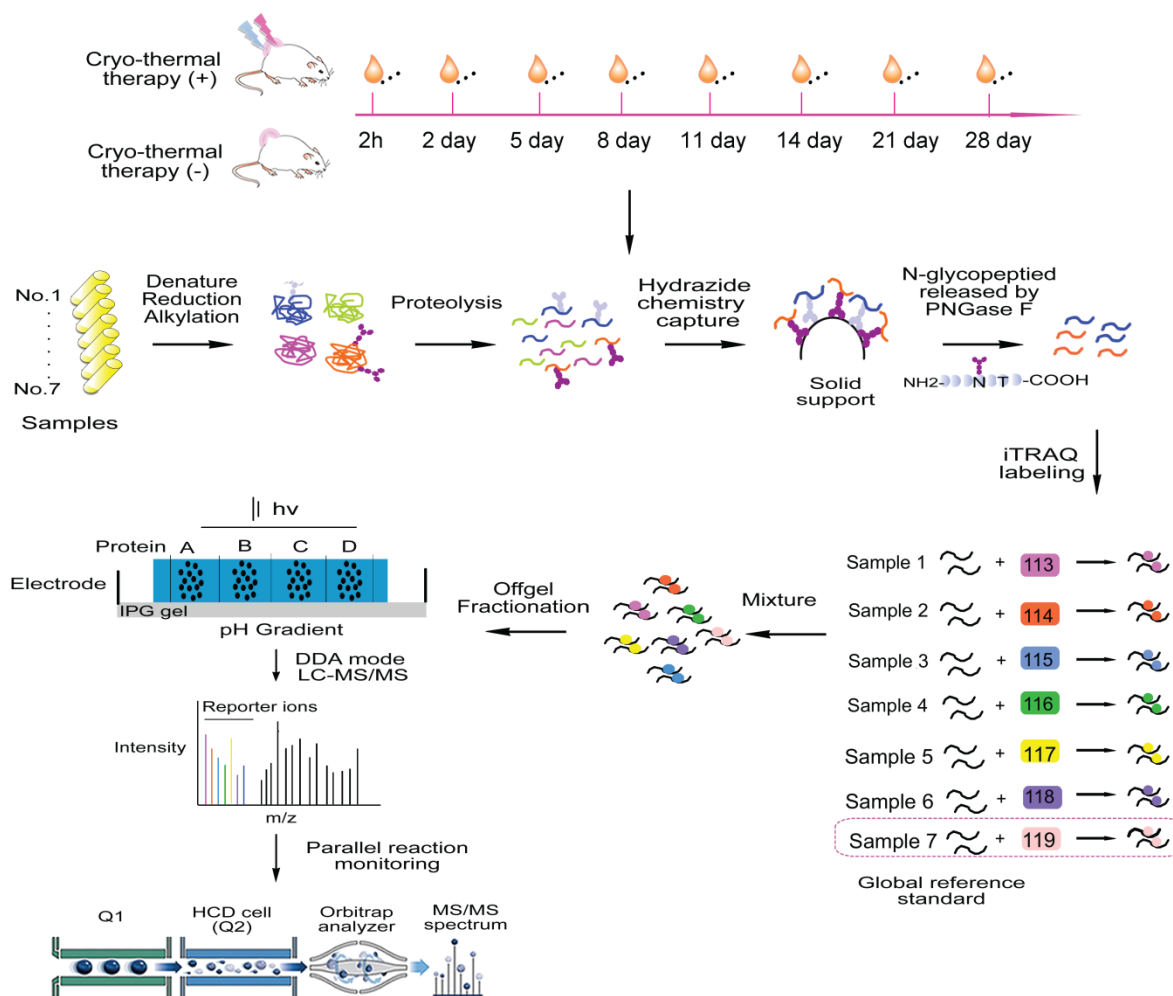
Figure 2. Proteomics analysis of serum glycoproteins from treated and untreated mice. 21 days after cell injection, mice underwent cryo-thermal or no treatment as control. Afterwards, mice were kept for another 2 h, 2, 5, 8, 11, 14, 21 and 28 days. For shotgun proteomics, serum were collected and pooled under each condition. After protein denaturation, reduction and alkylation, pooled sera were then digested to peptides. Subsequently, glycopeptides were captured by the hydrazide solid phase and cleaved by PNGase F enzyme. The released N-glycosylated peptides were than labeled with 8-plex iTRAQ reagent and mixed for subsequent off-gel pre-fractionation. N-glycosylated peptides extracted from healthy mice were labeled as the global reference. Each fraction was then subjected to LC-MS/MS for protein identification and quantification. Database search and analysis were performed in TPP and significant candidates were verified using quantitative PRM method for target analysis.
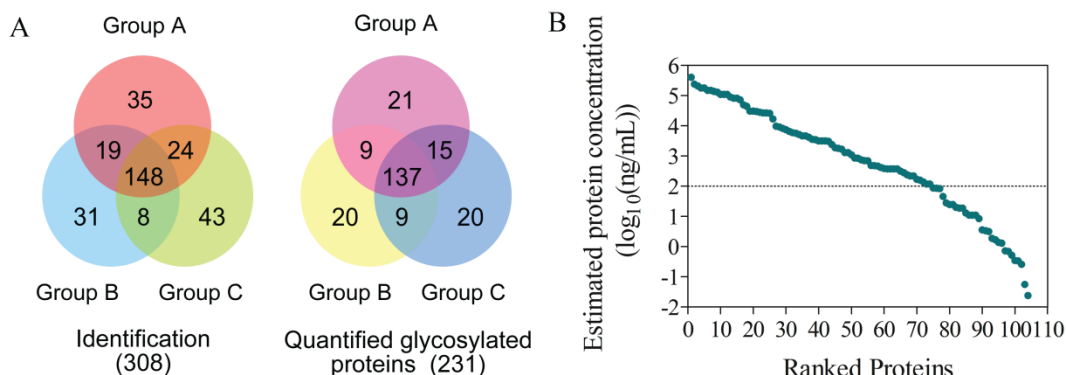

Figure 3. Proteomics identification and quantification. (A) The overlap of glycoproteins identified and quantified in three groups. (B) The estimated protein concentration in serum for those identified proteins, spanning 7 orders of magnitude.
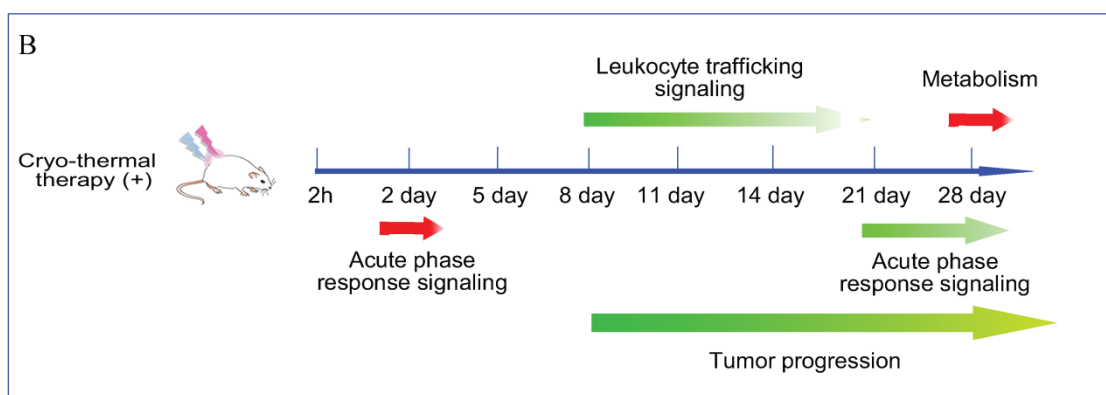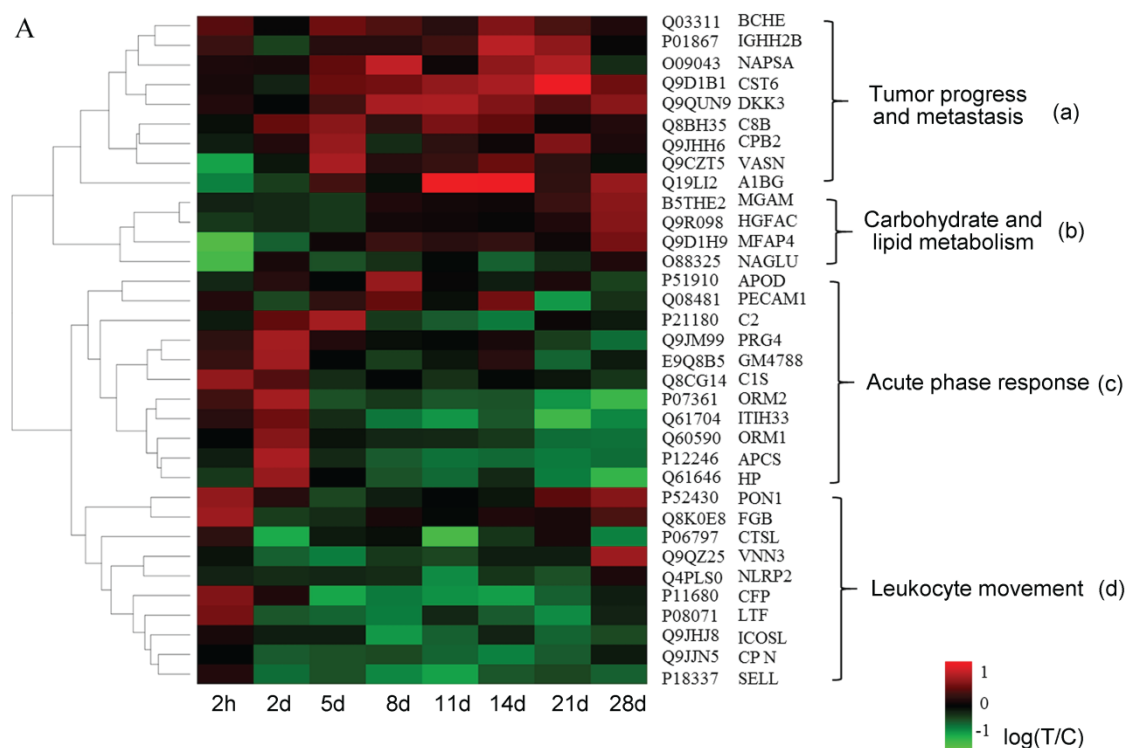
Figure 4. Quantitative time course measurement of induced proteome changes. (A) The unsupervised hierarchical clustering of significant proteins' changes over time course. The dendrogram generated represents the clustering of proteins (a-d). Biological process enrichment is based on IPA functional annotation. (B) The schematic graph of systematic response regulated in a time resolved pattern. Arrows in red represented proteins up-regulated, while in green are proteins down-regulated or in dysregulation.

Target proteomics investigating the function of acute phase response in anti-tumor activity.

To better understand how acute phase response acts in the anti-tumor activity, PRM based targeted proteomics validation on significant proteins was carried out in the following study. 5-6 mice under treated or control condition over 8 time points from the same sample as shotgun proteomics were analyzed, ending up with a total of 94 serum samples. Peptides used for target analysis were selected from previous shotgun proteomics via the following criteria: 1) N-glycosylated with fully tryptic termini, 2) commonly detected across all samples, and 3) doubly charged preferred. As a quality control, we spiked a commercially available standard angiotensin peptide in each enriched sample to evaluate the instrument performance. Additional File 7: Figure S5 showed that most of the coefficient variances (CV) of the angiotensin intensity under each condition were below 20%, and the CV value among different conditions was 22%, suggesting a good performance of instrument operation. Relative protein abundance of treat and untreated mice were expressed as fractions of the normalized value of the healthy mice which was set to 1 (base line). This PRM-based target analysis allowed us to conduct comprehensive validation of proteins in multiple biological replicates without pooling, which is not suitable for traditional approaches as western blot and ELISA, due to

limitations from time-consuming and antibody dependence.

Cryo-thermal therapy induced an "acute" phase response

First, we performed PRM analysis upon significant proteins involved in acute phase response, namely APCS, HP, ITIH3, ORM1, ORM2, ORM3, and PRG4, and they are defined as acute phase proteins (APPs). ORM2 and HP were quantified with an identical significant pattern as shotgun proteomics. Proteins such as ORM1, ORM3, APCS, ITIH3 and PRG4 were found to be significantly regulated at more time points in PRM analysis (Additional File 6: Table S6, Figure 5).

These proteins revealed a remarkable difference between treated and control mice. In particular, in control mice, these proteins persistently expressed at a significantly higher level than healthy mice and rapidly elevated to peak during the late stage of tumor development. A similar high expression was observed in treated mice 2 h post therapy, however, such expression peaked on the 2nd day, much higher than that of the control mice. Notably, the peak expression was transient (Figure 5, Additional File 7: Figure S6A). Although termed as "acute", such

response could turn into chronic upon persistent stimuli [36]. In this case, the persistent expression of APPs indicated that mice without treatment were involved in a long lasting inflammatory environment during tumor development. By contrast, cryo-thermal therapy rapidly drove a much stronger, but "acute" inflammatory response, breaking the chronic environment. Additionally, chronic inflammation is characterized by the disrupted leukocyte trafficking at inflamed sites [37]. In our study, SELL, an adhesion molecule mediating the leukocyte trafficking from bloodstream to inflamed sites [38, 39], was quantitatively analyzed using PRM, resulting in a similar pattern to shotgun proteomics (Additional File 6: Table S6). Compared to healthy, it constantly stayed at a much higher level in untreated mice (Figure 5), suggesting the persistent accumulation of inflammatory cells within tumor, and supporting the chronic inflammation mentioned above. By contrast, SELL was significantly down-regulated and gradually reduced to the base level during the late time points post therapy (Figure 5). This finding was consistent with the observed resolution of acute phase response in treated mice.
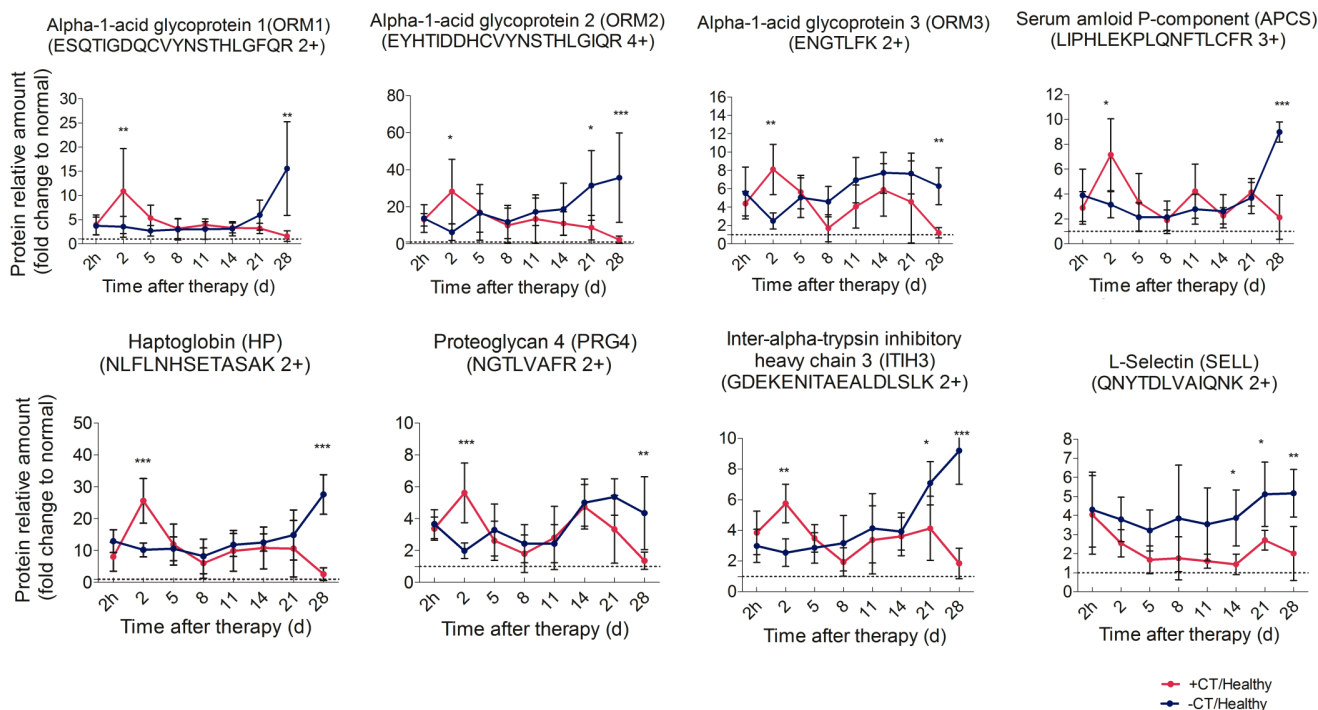

Figure 5. Time course verification of proteins associated with acute phase response and leukocyte activity using parallel reaction monitoring. Individual peptide's abundance was used as a proxy of protein's abundance. Peptide's abundance in mice treated and untreated was divided by its corresponding partner in healthy mice and plot over time. The dash line represents the protein expression level in healthy mice. Data are shown as mean ± SD. *p < 0.05, **p < 0.01, ***p < 0.001 by two-way ANOVA with the Bonferroni correction. n=5~6 for each condition, except that on the 28th day, only 3 mice left in the control group.
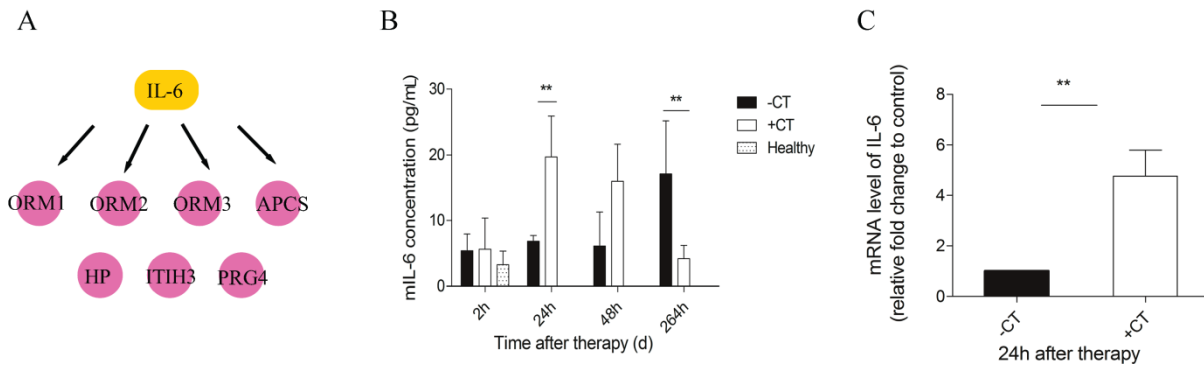
Figure 6. IL-6 was elevated in serum and local tumor site in a short time after therapy. (A) IL-6 was identified as the upstream regulator of acute phase proteins. (B) The amount of IL-6 in serum was measured by ELISA. (C) The expression of IL-6 within tumors was examined with RT-PCR. Data are shown as mean ± SD. **$p < 0.01$, by (B) two-way ANOVA with the Bonferroni correction; n=3 with two replicates assay. (C) Student t test. Triple replicates assay.

"Acute" interleukin-6 was induced by cryo-thermal therapy

Next, we carried out a network analysis on these APPs using IPA. Interestingly, interleukin-6 was identified as the key upstream regulator of these proteins (Figure 6A), indicating its significant role in inducing acute phase response. To further confirm this assumption, first, IL-6 levels in serum and within tumor were examined via ELISA and RT-PCR. As a result, IL-6 in circulation maintained at a persistent high level in control mice relative to healthy and even extensively increased on the 11th day (Figure 6B). However, cryo-thermal therapy immediately stimulated a considerable expression of IL-6 in serum and within local tumor on the 1st day, much stronger than mice untreated (Figure 6B, Figure 6C), whereas started to decline on the 2nd day and returned to a similar level as the healthy mice (Figure 6B). These findings are consistent with the APPs expression profiles. Next, prior to its peak expression, we neutralized IL-6 with IL-6 antibody *in vivo* 3 and 24 h post therapy. Serum was collected 2 days post therapy to examine the expression of APPs. Among APPs, ORM, APCS and HP are well documented in researches [40-42]. In addition, ORM1, ORM2 and ORM3 belong to the same family and ORM1 was identified with the most confident peptides in shotgun and PRM target proteomics compared to ORM2 and ORM3. In this case, ORM1, APCS and HP are selected. Western blot analysis showed that their expressions are significantly down-regulated after IL-6 neutralization (Figure 7). All these results indicated that "acute" activation of interleukin-6 was stimulated by cryo-thermal therapy, inducing the "acute" phase response.

"Acute" response could temper the Th2 immunosuppressive environment

As described, with the accumulating tumor burden, the expression of APPs steeply raised to the most on the last day (Figure 5), indicating the most severity of chronic inflammation. Chronic inflammation is associated with immunosuppression in many tumors [43], predominately induced by tumor infiltrating Tregs to suppress effector T cells and prevent tumor against immune surveillance [44]. The interaction of ICOS /ICOSL can boost Tregs activation, proliferation, and survival [45-47]. In addition, ICOSL could trigger the expression of immunosuppressive Th2 cytokines, such as IL-4, IL-5 and IL-13[48, 49]. Here, both shotgun proteomics discovery and PRM validation analysis revealed that ICOSL was significantly overexpressed during the late stage of tumor development, whereas it always stayed around the base line under "acute" response (Figure 8). This observation suggested that the Th2 immunosuppression may be attenuated by the cryo-thermal therapy induced "acute" response and thus the activation of anti-tumor immunity was favored.

"Acute" response could elicit innate and Th1 adaptive anti-tumor immunity

Since "acute" is a remarkable profile of cryo-thermal therapy, which leads to the attenuation of immunosuppression, we then interested in how this "acute" signature could benefit the anti-tumor immunity. We further evaluated proteins significantly expressed in the timeframe of "acute" response (2nd to 5th day post therapy) in shotgun proteomics. These proteins include CPB2, CTSL, C2, C8B, CFP, DPP4, MUP3, GRM7, VNN3 and VASN. Interestingly, among them, C2, C8B, CFP are involved in the activation of complement system; CTSL and DPP4 are responsible for T cell activation. All of them appear to regulate innate and adaptive immunity. Hence, we performed PRM target analysis to further examine these proteins. As a result, the significant expression of C2, C8B and CTSL, DPP4 were well in line with the shotgun proteomics (Table S6).

Particularly, C2 is the central regulator of classic and lectin complement pathways, and C8B is the component of terminal membrane attack complex (MAC) for cell lysis. These two proteins were reported to play critical roles in tumor cell clearance through phagocytosis and cell lysis, triggering innate immunity [50, 51]. In consistent, both proteins were shown being significantly up-regulated on the 5th day after treatment and returned to the base line, which is in agreement with the "acute" response profile. On the other hand, under chronic inflammation in untreatedmice, these proteins were shown to stay around the base level (Figure 8). All these observations implied that "acute" phase response could re-activate the impaired complement system under chronic inflammation and benefit anti-tumor innate immunity.
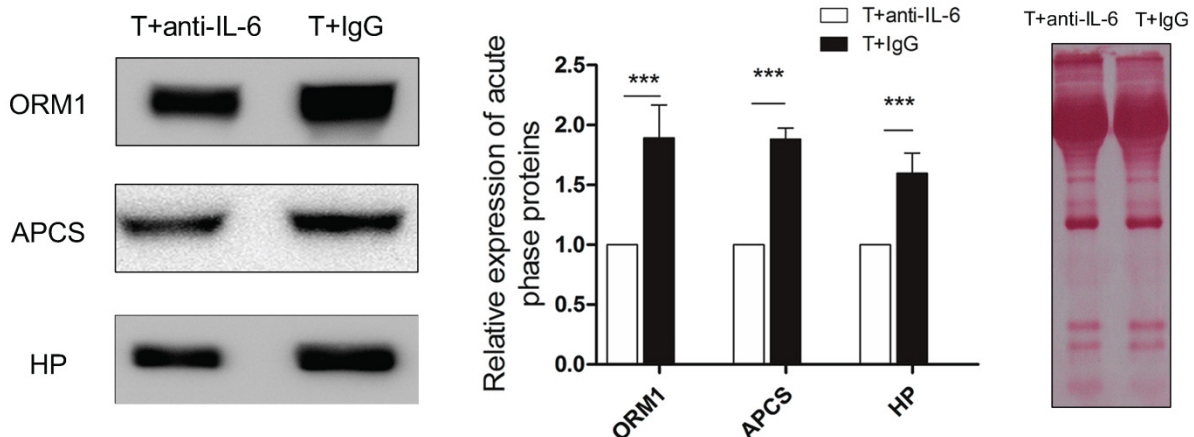

Figure 7. The expression of three acute phase proteins after IL-6 neutralization. Mice were injected intraperitoneally with mouse anti-IL-6 Ab 3 and 24 h post cryo-thermal therapy and sacrificed on the 2nd day. Serum was collected for western blot analysis. Protein amount was evaluated and visualized with Ponceau S. Blots were evaluated with Quantity One 1-D. Results are expressed as relative pixel intensity normalized with control group. Data are shown as mean ± SD. ***p < 0.001 by student t test. n=3 with three technical replicates.
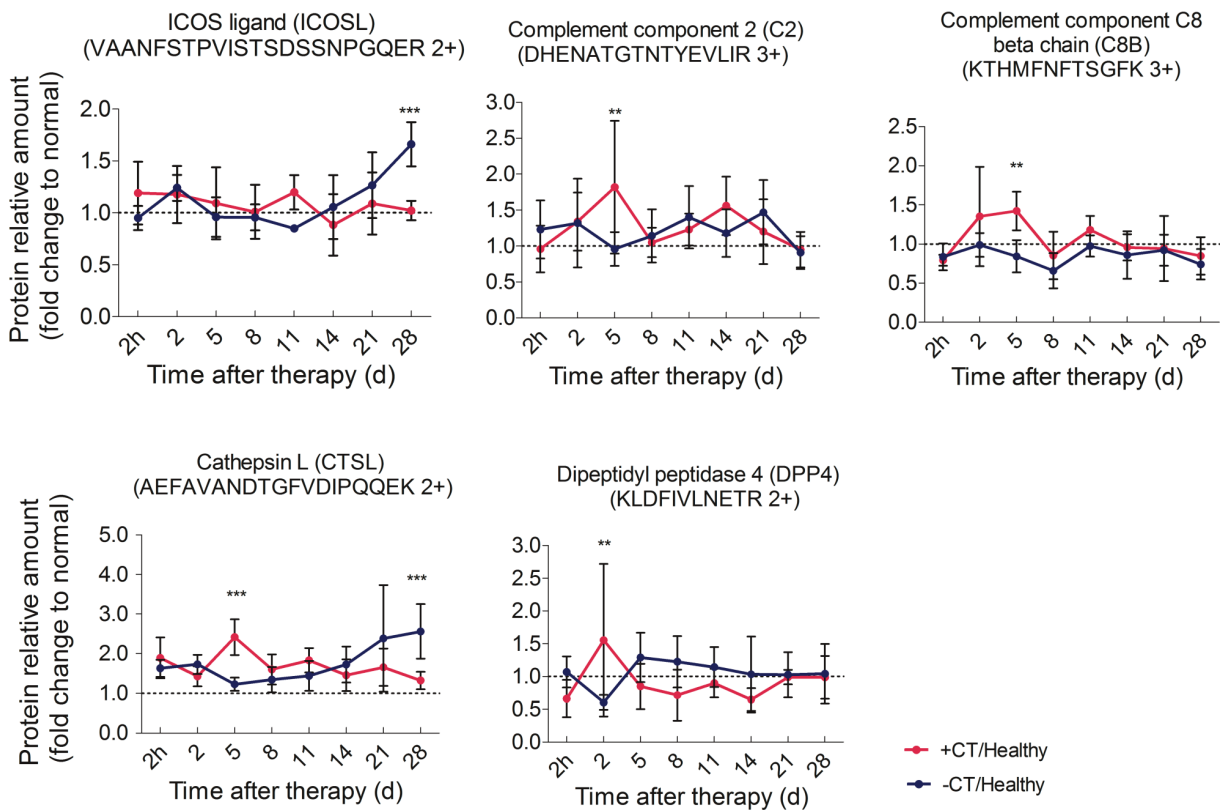

Figure 8. Time course verification of proteins associated with complement system and adaptive immunity using parallel reaction monitoring. The dash line represents the protein expression level in healthy mice. Data are shown as mean ± SD. **p < 0.01, ***p < 0.001 by two-way ANOVA with the Bonferroni correction. n=5~6 for each condition, except that on the 28th day, only 3 mice left in the control group.
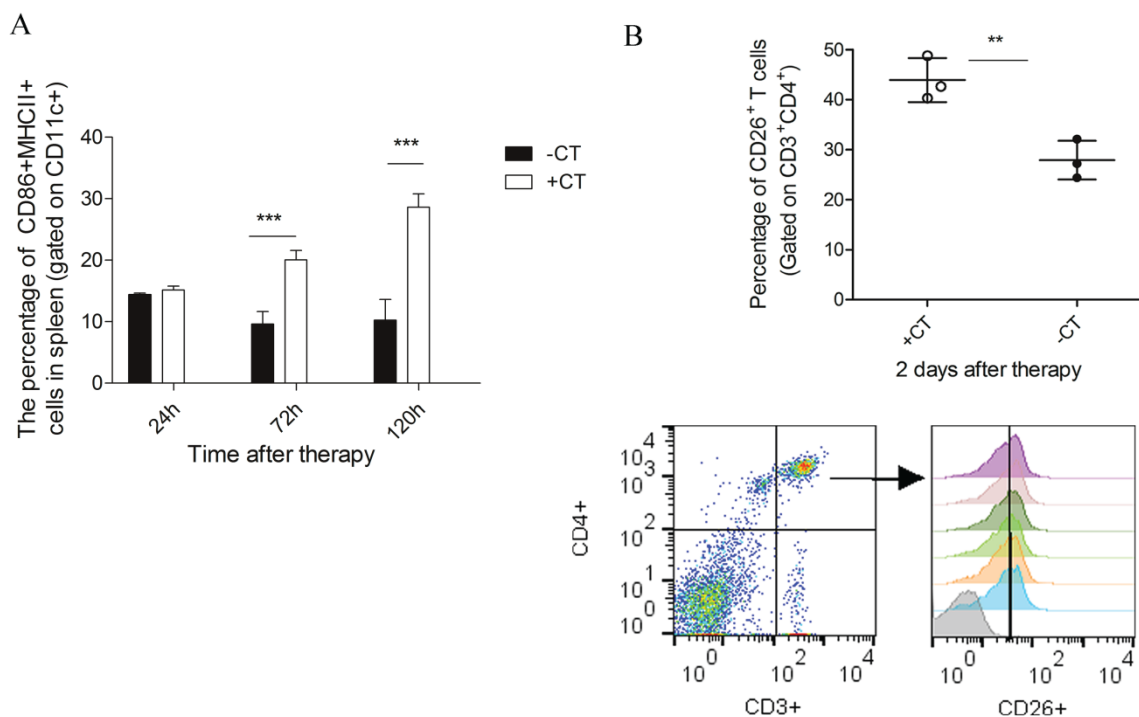
Figure 9. The maturation of DCs and activation of CD4+CD26+ T cells. (A) The percentage of CD86+MHCII+ DCs, gated on CD11c+. Lymphocytes were isolated from spleens 1 day, 3 day and 5 day post therapy and stained with the following Abs: anti-mouse-CD11c, anti-mouse- MHCII and anti-mouse-CD86. (B) The percentage of CD26+ T cells gated on CD3+CD4+. Lymphocytes were isolated from spleen on the 2nd day post therapy and stained with the following Abs: anti-mouse-CD3, anti-mouse-CD4 and anti-mouse-CD26. Data are shown as mean ± SD. **p < 0.01, ***p<0.001, by student t test, n=3.

In addition, CTSL was also observed up-regulated on the 5th day after therapy (Figure 8). CTSL plays important roles in antigen processing and maturation of antigen presenting cells (APCs) [52]. Such up-regulation suggested a possible maturation of APCs (like dendritic cells). Therefore, we performed flow cytometry to examine the maturation of dendritic cells in spleens of treated mice. As a result, matured DCs (CD11c+CD86+MHCII+) showed a significant increase on the 3rd day after therapy and was even higher on the 5th day, while it remained at a relative low level in the untreated mice (Figure 9A).

Concomitant with the "acute" response, DPP4 (known as CD26), with a soluble form in circulating system [53], was also shown up-regulated on the 2nd day after therapy and returned to the base level afterwards (Figure 8). CD26 is a maker of T cell activation which is highly expressed in the activated and antigen-reactive memory T cells. CD26high T cell could produce T-helper 1 (Th1) cytokines to elicit type-1 anti-tumor response (CD4+CD26+ T cell) or exert cytotoxic T lymphocyte activity (CD8+CD26+ T cell) [54-56]. The up-regulation of CD26 on the 2nd day suggested that more T memory cells were activated and proliferated upon "acute" response. To further confirm this suggestion, we performed flow cytometric analysis upon lymphocytes isolated from splenocytes 2 days post therapy. As a result, we found a strikingly increased percentage of CD4+CD26+ T cell

(Figure 9B) as compared to that of untreated mice. Therefore, these results confirmed that more CD4+ memory T cells were activated and proliferated upon "acute" response. By this manner, these cells could potentially serve as Th1 cells to initiate and amplify the adaptive immunity against tumor.

Since we observed the maturation of DCs and proliferation of Th1 memory T cells, we next examined the secretion of Th1 cytokines (IL-12 and IFN-γ) to further investigate whether protective Th1 adaptive immunity was activated under "acute" response. IL-12, naturally produced by dendritic cells, is important in directing the development of Th1 cells [57]. The source of IFN-γ is restricted to CD4+ Th1 cells, once antigen-specific immunity develops [58]. Hence, we examined their splenic expression on the 3rd day post therapy using RT-PCR. As shown in Figure 10, both IL-12 and IFN-γ exhibited the highest expression after the therapy, while in the untreated mice, their expression were inhibited compared to both healthy and treated mice. Therefore, the protective T helper type 1 immune response appeared to be activated after the therapy.

In summary, we suggested that "acute" response could elicit innate and Th1 adaptive immunity, reversing the tumor-mediated immunosuppressive environment toward an anti-tumor hub.
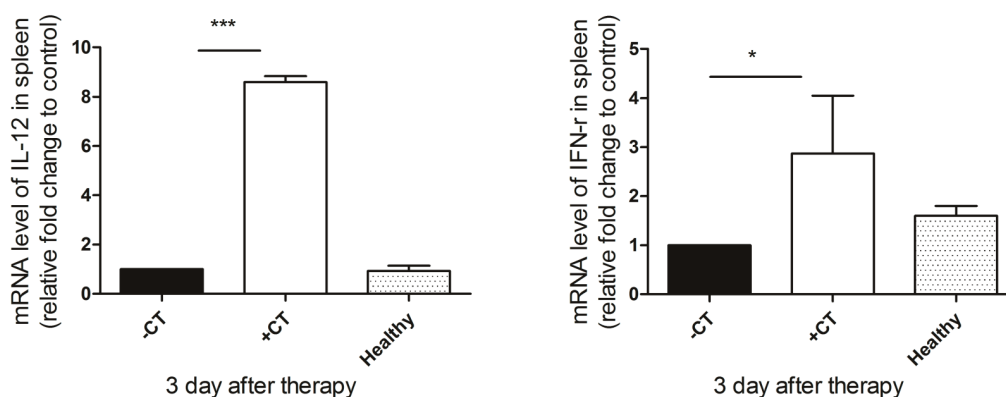
Figure 10. The secretion of Th1 cytokines on the 3rd post therapy. Spleens were extracted on the 3rd post therapy and the expression of IL-12 and IFN-γ were examined by RT-PCR. (A) The expression of IL-12. (B) The expression of IFN-γ. Data are shown as mean ± SD. *p < 0.05, ***p < 0.001 by student t test. Triple replicates assay.

"Acute" environment could benefit the upregulation of tumor metastatic inhibitory proteins

In addition to the strongly stimulated "acute" response by cryo-thermal therapy, tumor metastasis inhibition was also observed (Figure 1D). We then ask how such "acute" environment affects tumor metastasis. Here, tumor associated proteins significantly changed in shotgun proteomics (CST6, DKK3, NAPSA, A1BG) were targeted using PRM. Another protein sLIFR, exhibiting a non-significant but high level after therapy in shotgun analysis, was also included for PRM analysis due to its role in tumor progression (Additional File 7: Figure S7). By PRM, all proteins were shown up-regulated during the late stage post therapy (Figure 11A, Additional File 7: Figure S6B). Notably, CST6 was reported as the inhibitor of CTSL [59], which is a lysosome protease and could be secreted to extracellular space to enhance tumor invasion and metastasis [60]. Hence, we also targeted CTSL in PRM and found its down-regulation post therapy, which is opposite to the pattern of CST6 (Figure 11A).

Among them, CST6 and DKK3 are well accepted tumor suppressor proteins [61-63]; soluble LIFR and NAPSA were reported with capability to arrest tumor growth and metastasis [64]; although A1BG shows controversial profiles in different cancers [65-68], it does associate with tumor progression. Interestingly, all of these up-regulated proteins localized in the extracellular space. Taken together, we proposed that the cryo-thermal therapy induced "acute" environment stimulates the expression of tumor progression and metastatic inhibitory proteins and further augment their secretion from host cells to circulation, which counteract the negative impact of chronic inflammation on cancer malignance and prevent tumor metastasis.

"Acute" response induced anti-tumor activity ended up with the recovery of host physiology

It is well accepted that excessive and uncontrolled inflammatory mediators would cause organ failure. In untreated mice, lung swelling was accompanied by the increasing tumor metastasis, indicating its disordered function. However, the lung size was similar to normal in post therapy mice (Figure 1D). In our shotgun proteomics analysis, we found a significant up-regulation of MFAP4 protein on the last day after therapy. MFAP4 was related to elastogenesis in lung. Deficiency of MFAP4 in mice was shown to develop a spontaneous loss of lung function [69, 70]. Therefore, we carried out PRM analysis on MFAP4 for further evaluation. As a result, MFAP4 was consistently expressed at a low level and decreased over time in response to tumor burden, while up-regulated and returned to the base line (Figure 11B) post therapy, which is generally consistent with shotgun proteomics results (Table S6). Therefore, the malfunction of lung upon tumor progression could be reversed by the cryo-thermal therapy under a mechanism of the anti-tumor activity mediated by the "acute" response.

In addition, chronic inflammation could result in changes of lipid metabolism and decreased gluconeogenesis [71]. Hence, significant proteins associated with glucose and lipid metabolism were examined using PRM. These proteins are MUPs, MGAM and PON1 (Figure 11B, Additional File 7: Figure S6C). Similar to that in the shotgun proteomics analysis (Additional File 6: Table S6), these proteins were shown to remain at low levels and decreased over time under chronic environment. However, they were increased to the normal level after cryo-thermal therapy. Overall, it is suggested that the metabolism was distorted during tumor progression, while it could successfully be restored under "acute" environment.
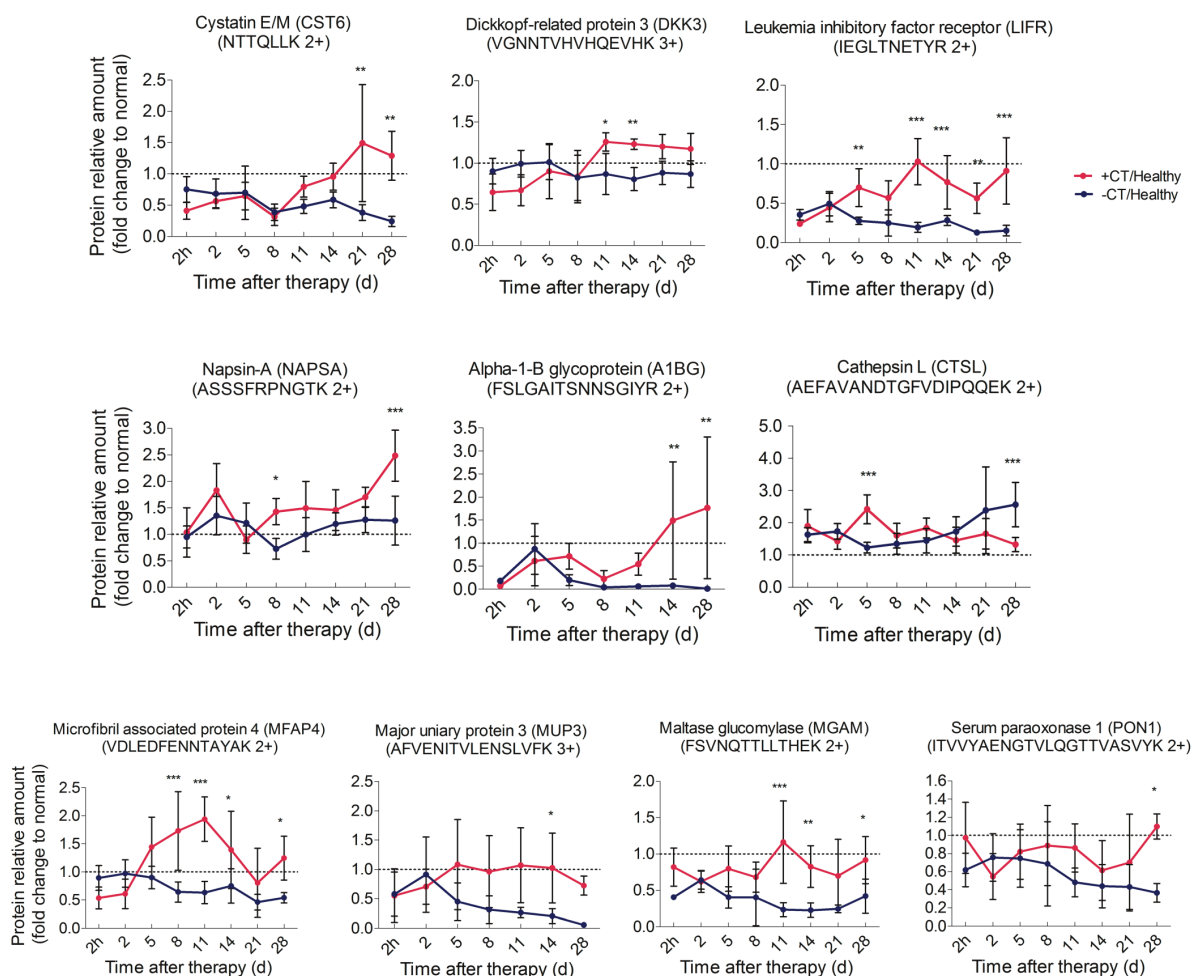
Figure 11. Time course verification of proteins associated with tumor progression and metabolism using parallel reaction monitoring. The dash line represents the protein expression level in healthy mice. Data are shown as mean ± SD. *$p < 0.05$, **$p < 0.01$, ***$p < 0.001$ by two-way ANOVA with the Bonferroni correction. n=5~6 for each condition, except that on the 28th day, only 3 mice left in the control group.

The strongest and unique "acute" environment induced by cryo-thermal therapy stimulated the most effective anti-tumor immune response

As described above, "acute' environment is suggested to be the key driver to switch tumor microenvironment from immunosuppressive to immunostimulatory state. In addition, the combination of cryo/hyperthermia showed prolonged survival rate and reduced metastasis compared with cryotherapy or hyperthermia alone. In this case, we are interested in the "acute" profile in different therapeutics and the relationship with anti-tumor immunity. First, we compared the expression of three well documented APPs (ORM1, APCS and HP) [40-42] in serum 2 days post different treatments on tumors, which are 1) cryo-thermal therapy, 2) cryotherapy, 3) hyperthermia and 4) control without treatment. Western blot analysis showed that cryo-thermal therapy induced the strongest acute response as indicated by the highest

expression of selected APPs (Figure 12). As described above, "acute" response could lead to DC maturation and Th1 adaptive immune response in early stage. To better compare the immunological effect stimulated by "acute" response, we next tested the adaptive immune response in later stage. As a result, cryo-thermal therapy elicited a significant protective immune response with the most accumulated CD8+ and CD4+ T lymphocytes in spleen 14 days post treatment (Figure 13A, 13B). In addition, the immunosuppressive state was most inhibited indicated by the maximally reduced MDSC (Gr1+CD11b+) (Figure 13C). These findings suggested that as a combination of cryo/hyperthermia, cryo-thermal therapy established the strongest "acute" environment, which could benefit the stimulation of the most pronounced anti-tumor adaptive immune response.

Moreover, to delineate the "unique" immunological effect of cryo-thermal therapy on tumor tissues, we further examined the "acute" profile and corresponding immune response in

heathy mice under this specific therapy. As shown, cryo-thermal on healthy mice (N+A) induced "acute" response; however, such "acute" pattern was much weaker than that applied on tumors (Figure 12). We assumed that the "danger" signal released from tumors could boost the host "acute" inflammation. In addition, cryo-thermal therapy induced the most pronounced protective T lymphocyte response on tumors, whereas it was not changed much in healthy mice, regardless of treatment or not, indicating that such immune response was not effectively stimulated

without the presence of antigen released from tumors (Figure 13A, 13B). As shown, MDSC, with remarkable immunosuppressive abilities in cancer, was largely reduced after cryo-thermal therapy on tumors; however, it was induced under "acute" response in healthy mice, which could quickly differentiate into mature myeloid cells predominantly participating in innate immune response, while have a minimal impact on the adaptive immune response [72] (Figure 13 C).
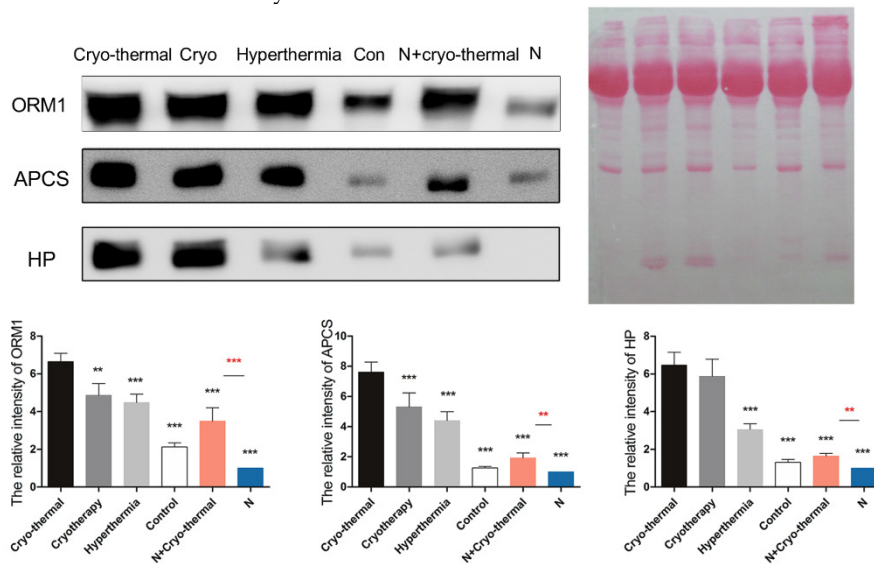

Figure 12. The expression of acute phase proteins through different energy-based therapeutics applied on tumors and healthy mice. Tumor bearing mice were treated with 1) cryo-thermal therapy, 2) cryotherapy, 3) hyperthermia and 4) control (no treatment). Healthy mice with and without cryo-thermal were set as another controls. 2 days post therapy, serum was collected for western blot analysis. Protein amount was evaluated and visualized with Ponceau S. Blots were evaluated with Quantity One 1-D. Results are expressed as relative pixel intensity normalized with healthy group. Data are shown as mean ± SD. **p<0.01, ***p < 0.001 by one way ANOVA with Dunnett's test and each group was compared with cryo-thermal therapy. Healthy mice with and without treatment were analyzed by student t test. n=3 with three technical replicates.
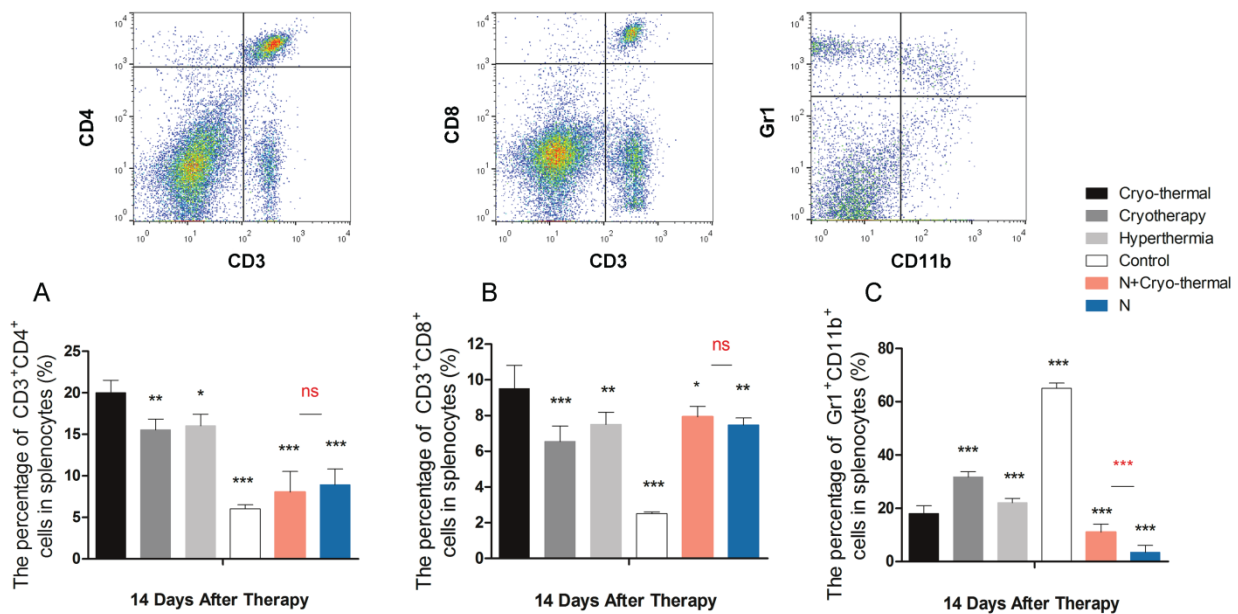

Figure 13. The protective adaptive immune response and immunosuppression arising from different energy-based therapeutics applied on tumors and healthy mice. Tumor bearing mice were treated with 1) cryo-thermal therapy, 2) cryotherapy, 3) hyperthermia and 4) control (no treatment). Healthy mice with and without cryo-thermal were set as another controls. Lymphocytes were isolated from spleens 14 days post therapy. (A) The percentage of CD3+CD4+ T lymphocytes. (B) The percentage of CD3+CD8+ cytotoxic T lymphocytes. (C) The percentage of Gr1+CD11b+ MDSC cells. Data are shown as mean ± SD. *p<0.05, **p<0.01, ***p < 0.001 by one way ANOVA with Dunnett's test and each group was compared with cryo-thermal therapy. Healthy mice with and without treatment were analyzed by student t test. n=3.

Taken together, we concluded that cryo-thermal therapy has a better immunological effect over cryo/hyperthermia alone and such effect was unique on tumors.

Discussion

Metastatic breast cancer remains a big challenge in clinical practice. Based on thermal therapeutic strategy, we previously developed the cryo-thermal therapy as an energy-based cancer intervention. This strategy has shown a good therapeutic efficacy with prolonged lifespan and reduced metastasis (Figure 1). In this study, serum glycoproteome comparison using shotgun proteomics analysis followed by PRM target validation was carried out to dissect the distinct protein profiles between treated and untreated mice on multiple samples (94) and time points (8), in order to better understand the molecular mechanism of the anti-tumor activity on a system-wide view. In general, targeted proteins exhibited consistent significant expression with that in shotgun proteomics, to some extent, the enhanced sensitivity and selectivity of PRM assay provides better quantitative information for some proteins, such as ORM1, ORM3, APCS, ITIH3, PRG4, SELL, MUP3, MGAM and MFAP4. More importantly, such high throughput target proteomics allowed us to validate proteins on a large scale (multiple samples and proteins), which was not suitable using traditional approaches such as western blot and ELISA, due to limitations from time-consuming and antibody dependence.

In this study, we found that "acute" response was strongly induced by cryo-thermal therapy with "acute" and high expression of a series of acute phase proteins and consequently reverse the tumor chronic pro-tumorigenic environment. "Acute' response is generally occurred as an immediate and evident inflammation in response to stress. In tumor progress, chronic environment is often induced with little visible inflammatory reaction, whereas it becomes apparent and severe upon extensive tumor expansion [73]. As the critical upstream regulator of acute response, IL-6 was also identified with an "acute" profile in our study, whose reduced level decreased the magnitude of "acute" response. Previously, "acute" IL-6 induced by adipose-derived stromal/stem cells has been proved to mediate the good therapeutic effects in acute lung injury [74]. In addition, fever-range thermal stress induced "acute" activation of IL-6 has been indicated with anti-tumor activity through boosting T lymphocyte trafficking [75-77] and amplifying the killing cytotoxic effector of CD8+ effector T cells toward tumor cells [78]. However, the sustained elevated IL-6 concentration in circulating has been observed in numerous cancers and is a prognostic indicator of poor outcome [79-81]. Hence we hypothesized that "acute" IL-6 induced "acute" response plays a key role in anti-tumor activity.

In this study, we proposed a model that IL-6 induced "acute" response could mediate anti-tumor activity in three aspects, which could interact with each other and result in the good therapeutic efficacy. They are 1) Th2 immunosuppressive response breaking, shifting pro-tumorigenic phenotype toward 2) tumoricidal innate and Th1 adaptive immunity activation and 3) up-regulation of tumor progression and metastatic inhibitors. The details were described below (Figure 14).

Cryo-thermal therapy, by applying through rapid freezing followed by heating, would result in severe thermal and mechanical stresses to local tumor. The severe stress could thus stimulate a rapid and vast generation of IL-6 through macrophages influx. Such "acute" activation of IL-6 rapidly induces the "acute" phase response, generating an "acute" microenvironment, and disrupting the chronic inflammation in tumor site. Such "acute" microenvironment restricts the expression of ICOSL around the baseline, well controlling the Th2 immunosuppressive response (like Tregs, IL-4, IL-5, and IL-13) induced by chronic environment and favoring a protective immunity hub. Under this "acute" environment, acute phase proteins (APPs) are up-regulated, facilitating the phagocytosis of tumor cells and clearance of injurious agents through opsonisation or secreted pathogen recognition receptors [36, 82]. In addition, complement system is also activated, further improving the clearance of damaged tumor cells through phagocytosis, and facilitating the lysis of invading tumor cells via the formation of the terminal membrane attack complex (MAC) [83] to release the metastatic risk. By such manner, anti-tumor innate immunity is initiated. Subsequently, complement system could drive the innate toward adaptive immunity to promote the anti-tumor immune response. It has been shown that its products, such as anaphylatoxins (C3a, C5a) [84, 85], C1q and C3 fragment [86-88] can directly induce dendritic cells (DCs) maturation and promote the development of effector T cells. This is in line with our observation that CTSL was up-regulated and more DCs were maturated on the similar day to complement system activation (3rd and 5th day). In addition, it has been reported that "acute" IL-6 could limit the activity of virus-specific Tregs, thereby facilitating the activity of virus-specific memory CD4+ T cells[89]. Consistently, in our study, an increased number of CD26+CD4+ memory T lymphocytes were activated and proliferated accompanied by the

"acute" response, favoring the Th1 anti-tumor adaptive immunity. To be noted, in our study, activated memory T cells appeared a bit earlier than the matured DCs augmentation (2nd day vs 3rd day). In fact, memory T cells have lower need of MHC-peptide

for activation than naïve T cells and response more fast and robust [90]. Such rapid response allows memory T to attack the tumor cells as early as possible. Furthermore, DC producing IL-12 contributes to the development of Th1 that generates high amount of IFN-γ to further promote Th1 polarization, while suppressing Th2 cell differentiation, favoring the protective Th1 adaptive immune response. Notably, "acute" response started to resolve with reduced production of IL-6, declined expression of APPs on 2nd day and less leukocyte trafficking. Such resolution is critical, not only to maintain the homeostasis of hostile environment, but also bridge the gap between innate and adaptive immunity for the optimal development of adaptive immunity [91].

What's more, "acute" micro-environment activated the secretion of tumor progression and metastatic inhibitory proteins by host cells to reduce metastasis. Finally, with the struggle of above three aspects, "acute" response induced by cryo-thermal therapy switches the Th2 immunosuppressive, pro-tumorigenic environment to a Th1 immunostimulatory, tumoricidal phenotype, protecting the host from accumulated tumor burden, reducing metastasis and recovering the host metabolism in the end.

To be noted, APPs studied in our work are relative high abundant proteins, which benefit their identification and quantification in cryo-thermal therapy and other biological events, like in cryotherapy or hyperthermia treatment of cancer. However, their "acute" profiles are markedly different. Cryo-thermal therapy induced the strongest "acute" response and elicited the most pronounced immunological effect compared to cryotherapy and hyperthermia alone. Moreover, cryo-thermal therapy on healthy tissue induced weaker "acute" response and failed to stimulate effective immunological effect
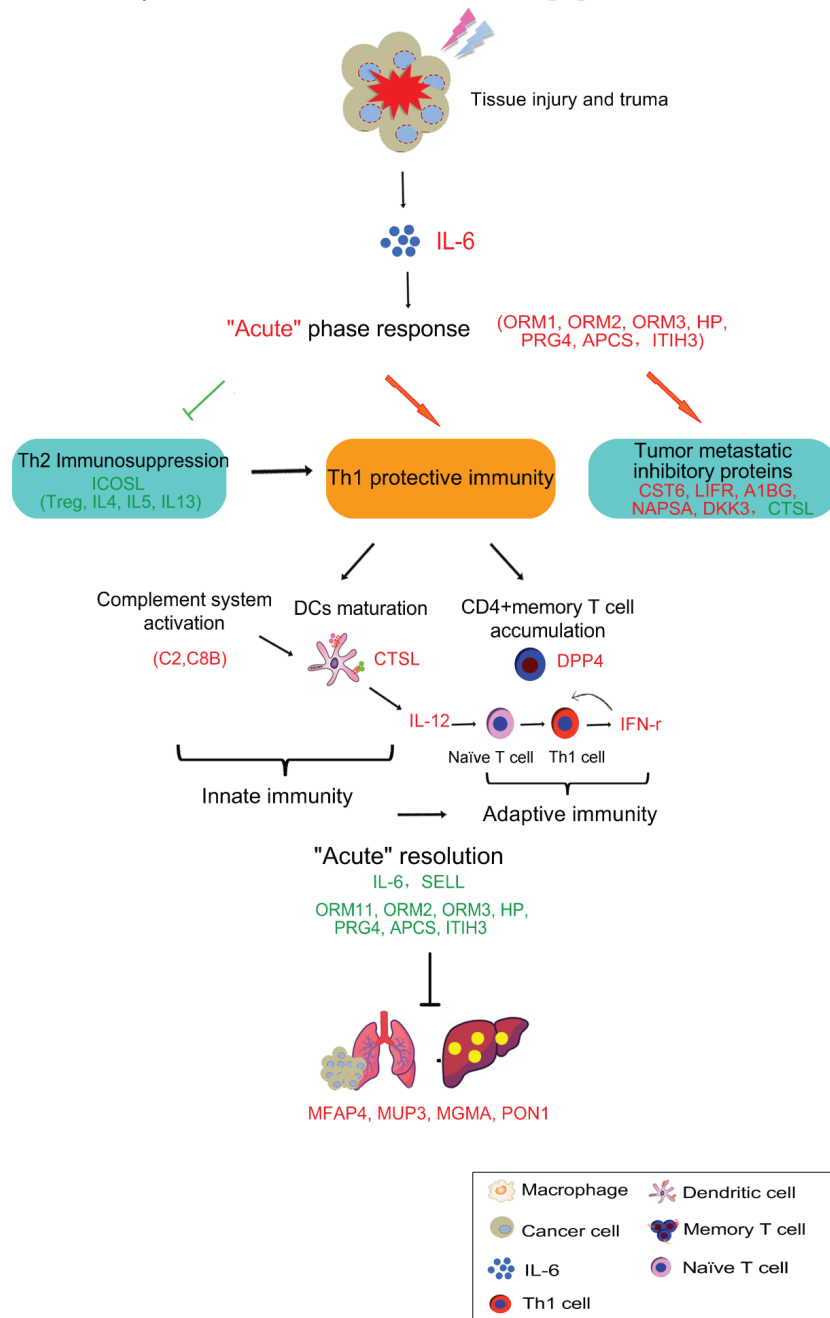

Figure 14. The schematic graph of "acute" response mediated anti-tumor activity induced by cryo-thermal therapy. The cryo-thermal therapy performed by rapid switch between freezing and heating causes a severe thermal and mechanical stresses to local tumor, leading a rapid and vast generation of IL-6 by macrophage influx. The "acute" IL-6 induced "acute" response could mediate anti-tumor activity in three aspects, which could interact with each other and enhance the anti-tumor effect. They are 1) Th2 immunosuppression breaking, 2) driving anti-tumor innate and Th1 adaptive immunity activation, characterized by complement system activation, more matured DCs and CD4+ memory T cell accumulation, as well as the secretion of Th1 cytokines to promote the differentiation of naïve T cells to Th1 cells, and 3) up-regulation of tumor progression and metastatic inhibitory proteins. In addition, "acute" resolution is critical, not only to maintain the homeostasis of hostile environment, but also bridge the gap between innate and adaptive immunity for the optimal development of adaptive immunity. Finally, "acute" response mediated anti-tumor activity leads to the recovered liver metabolism and normal physiological function. In addition, tumor recurrence is reduced and metastasis is inhibited. Proteins in red are up-regulated, green are down-regulated.

compared with tumors. In this case, we suggested that the magnitude of "acute" and the release of "danger" signals play a key role in determining the efficacy of anti-tumor immunity.

Conclusion

In summary, using comprehensive discovery proteomics analysis followed by target proteomics validation at a large scale sample size, we performed a system-based high throughput analysis to better understand the biological response induced by cryo-thermal therapy and reveal the stimulation of tumor-specific immunity at the molecular level. The cryo-thermal therapy induced strongest "acute" response helped boost systematic anti-tumor immune response in the host for a stronger immunogenicity environment, which enabled more effective cure of metastatic tumor.

Supplementary Material

Additional File 1:
Supplementary Table 1.
http://www.thno.org/v06p0773s1.xlsx
Additional File 2:
Supplementary Table 2.
http://www.thno.org/v06p0773s2.xlsx
Additional File 3:
Supplementary Table 3.
http://www.thno.org/v06p0773s3.xlsx
Additional File 4:
Supplementary Table 4.
http://www.thno.org/v06p0773s4.xlsx
Additional File 5:
Supplementary Table 5.
http://www.thno.org/v06p0773s5.xlsx
Additional File 6:
Supplementary Table 6.
http://www.thno.org/v06p0773s6.xlsx
Additional File 7:
Supplementary Figures.
http://www.thno.org/v06p0773s7.pdf

Abbreviations

A1BG: Alpha-1-B glycoprotein; APCs: Antigen presenting cells; APCS: Serum amyloid P-component; APPs: Acute phase proteins; C2: Complement component 2; C8B: Complement component 8, beta polypeptide; CFP: Complement factor properdin; CST6: Cystatin E/M; CTSL: Cathepsin L1; DDA: Data-dependent acquisition; DC: Dendritic cell; DKK3: Dickkopf-related protein 3; DMEM: Dulbecco's Modified Eagle's Medium; DPP4: Dipeptidyl-peptidase 4; FBS: Fetal bovine serum; FDR: False discovery rate; HCD: Higher-energy collisional dissociation; HP: Haptoglobin; ICOSL:

ICOS ligand; IL-4: Interleukin 4; IL-5: Interleukin 5; IL-6: Interleukin 6; IL-12: Interleukin 12; IL-13: Interleukin 13; IFN-γ: Interferon gamma; IPA: Ingenuity Pathway Analysis; iTRAQ: Isobaric tags for relative and absolute quantitation; MDSC: Myeloid-derived suppressor cells; MFAP4: Microfibrillar-associated protein 4; MGAM: Maltase-glucoamylase; MUP3: Major urinary protein 3; NAPSA: Napsin-A; ORM1: Alpha-1-acid glycoprotein 1; ORM2: Alpha-1-acid glycoprotein 2; ORM3: Alpha-1-acid glycoprotein 3; PON1: Serum paraoxonase/arylesterase 1; PRG4: Proteoglycan 4; PRM: Parallel reaction monitoring; SELL: L-selectin; sLIFR: Soluble leukemia inhibitory factor receptor; SRM: Selected reaction monitoring; TAMs: Tumor associated macrophages; TFE: Trifluoroethanol; Th1: T-helper 1; TPP: Trans-Proteomic Pipeline; Tregs: T regulatory cells

Author contributions

TX, PL, WY, and RLM conceived and designed the research. LXX was the project leader. TX conducted the experiments and data analysis. TX and WY wrote the manuscript. YZ and LY helped design and modify the glycocapture and iTRAQ experiments. LY helped analysis the MS data. KL performed the RT-PCR experiments.

Competing Interests

The authors have declared that no competing interest exists.

References

1. Torre LA, Bray F, Siegel RL, Ferlay J, Lortet-Tieulent J, Jemal A. Global cancer statistics, 2012. CA: a cancer journal for clinicians. 2015; 65: 87-108.
2. Hall-Craggs MA, Vaidya JS. Minimally invasive therapy for the treatment of breast tumours. European journal of radiology. 2002; 42: 52-7.
3. Vogl TJ, Farshid P, Naguib NN, Zangos S. Thermal ablation therapies in patients with breast cancer liver metastases: a review. European radiology. 2013; 23: 797-804.
4. Gage AM, Montes M, Gage AA. Destruction of hepatic and splenic tissue by freezing and heating. Cryobiology. 1982; 19: 172-9.
5. Hines-Peralta A, Hollander CY, Solazzo S, Horkan C, Liu ZJ, Goldberg SN. Hybrid radiofrequency and cryoablation device: preliminary results in an animal model. Journal of vascular and interventional radiology : JVIR. 2004; 15: 1111-20.
6. Kuz'menko A, Todor I, Mosienko V. The effect of the combined use of cryosurgery and hyperthermia on an experimental tumor process. Eksperimental'naia onkologiia. 1989; 12: 60-1.
7. Osinsky SP, Rikberg AB, Bubnovskaja LN, Trushina VA. Tumour pH drop after cryotreatment and enhancement of hyperthermia antitumour effect. Int J Hyperthermia. 1993; 9: 297-301.
8. Sun J, Zhang A, Xu LX. Evaluation of alternate cooling and heating for tumor treatment. Int J Heat Mass Transf. 2008; 51: 5478-85.
9. Cai Z, Song M, Zhang A, Sun J, Xu LX. Numerical simulation of a new probe for the alternate cooling and heating of a subcutaneous mouse tumor model. Numerical Heat Transfer, Part A: Applications. 2013; 63: 534-48.
10. Liu J, Ren X, Liu P. Study of Anti-tumor Immunity Induced by Local Thermal Stimulation Using 4T1 Murine Breast Cancer Model. 2013 International Conference on Biological, Medical and Chemical Engineering. 2013: 57-62.
11. Sun J, Xu C, Wei G, Sun X, Liu P, Zhang A, et al. Tumor treatment system with alternate cooling and heating-preliminary results in an animal model. World Congress on Medical Physics and Biomedical Engineering, September 7-12, 2009, Munich, Germany: Springer; 2009: 337-40.
12. Wei C, Shen E, Sun D, Zhang A, Sun J, Hu B. Assessment of alternated cooling and heating treatment by US combined CEUS in the VX2 rabbit liver tumor model. Chinese Sci Bull. 2014; 59: 865-73.
13. Webb H, Lubner MG, Hinshaw JL. Thermal ablation. Seminars in roentgenology. 2011; 46: 133-41.
14. Skitzki JJ, Repasky EA, Evans SS. Hyperthermia as an immunotherapy strategy for cancer. Current opinion in investigational drugs. 2009; 10: 550-8.
15. Sabel MS, Nehs MA, Su G, Lowler KP, Ferrara JL, Chang AE. Immunologic response to cryoablation of breast cancer. Breast cancer research and treatment. 2005; 90: 97-104.
16. Shen Y, Liu P, Zhang A, Xu LX. Study on tumor microvasculature damage induced by alternate cooling and heating. Ann Biomed Eng. 2008; 36: 1409-19.
17. Dong J, Liu P, Xu LX. Immunologic response induced by synergistic effect of alternating cooling and heating of breast cancer. Int J Hyperthermia. 2009; 25: 25-33.
18. Liu P, Ren X, Xu LX. Alternate Cooling and Heating Thermal Physical Treatment: An Effective Strategy Against MDSCs in 4T1 Mouse Mammary Carcinoma. ASME 2012 Summer Bioengineering Conference: American Society of Mechanical Engineers; 2012: 937-8.
19. Aebersold R, Mann M. Mass spectrometry-based proteomics. Nature. 2003; 422: 198-207.
20. Li XJ, Hayward C, Fong PY, Dominguez M, Hunsucker SW, Lee LW, et al. A blood-based proteomic classifier for the molecular characterization of pulmonary nodules. Science translational medicine. 2013; 5: 207ra142.
21. Gallien S, Bourmaud A, Kim SY, Domon B. Technical considerations for large-scale parallel reaction monitoring analysis. J Proteomics. 2014; 100: 147-59.
22. Ronsein GE, Pamir N, von Haller PD, Kim DS, Oda MN, Jarvik GP, et al. Parallel reaction monitoring (PRM) and selected reaction monitoring (SRM) exhibit comparable linearity, dynamic range and precision for targeted quantitative HDL proteomics. Journal of proteomics. 2015; 113: 388-99.
23. Peterson AC, Russell JD, Bailey DJ, Westphall MS, Coon JJ. Parallel reaction monitoring for high resolution and high mass accuracy quantitative, targeted proteomics. Mol Cell Proteomics. 2012; 11: 1475-88.
24. Anderson NL, Anderson NG. The human plasma proteome: history, character, and diagnostic prospects. Mol Cell Proteomics. 2002; 1: 845-67.
25. Zhang H, Li XJ, Martin DB, Aebersold R. Identification and quantification of N-linked glycoproteins using hydrazide chemistry, stable isotope labeling and mass spectrometry. Nature biotechnology. 2003; 21: 660-6.
26. Dennis JW, Granovsky M, Warren CE. Glycoprotein glycosylation and cancer progression. Biochim Biophys Acta. 1999; 1473: 21-34.
27. Gornik O, Royle L, Harvey DJ, Radcliffe CM, Saldova R, Dwek RA, et al. Changes of serum glycans during sepsis and acute pancreatitis. Glycobiology. 2007; 17: 1321-32.
28. Saldova R, Royle L, Radcliffe CM, Abd Hamid UM, Evans R, Arnold JN, et al. Ovarian cancer is associated with changes in glycosylation in both acute-phase proteins and IgG. Glycobiology. 2007; 17: 1344-56.
29. [Internet] A combined UniProtKB/Swiss-Prot and UniProtKB/VarSplic mouse database. ftp://ftp.uniprot.org/pub/databases/uniprot/current_release/knowledgebase/complete/.
30. [Internet] cRAP. ftp://ftp.thegpm.org/fasta/cRAP.
31. Vizcaino JA, Deutsch EW, Wang R, Csordas A, Reisinger F, Rios D, et al. ProteomeXchange provides globally coordinated proteomics data submission and dissemination. Nature biotechnology. 2014; 32: 223-6.
32. MacLean B, Tomazela DM, Shulman N, Chambers M, Finney GL, Frewen B, et al. Skyline: an open source document editor for creating and analyzing targeted proteomics experiments. Bioinformatics. 2010; 26: 966-8.
33. Zien A, Aigner T, Zimmer R, Lengauer T. Centralization: a new method for the normalization of gene expression data. Bioinformatics. 2001; 17 Suppl 1: S323-31.
34. Farrah T, Deutsch EW, Omenn GS, Campbell DS, Sun Z, Bletz JA, et al. A high-confidence human plasma proteome reference set with estimated concentrations in PeptideAtlas. Mol Cell Proteomics. 2011; 10: M110 006353.
35. Harel M, Oren-Giladi P, Kaidar-Person O, Shaked Y, Geiger T. Proteomics of microparticles with SILAC Quantification (PROMIS-Quan): a novel proteomic method for plasma biomarker quantification. Mol Cell Proteomics. 2015; 14: 1127-36.
36. Gruys E, Toussaint MJ, Niewold TA, Koopmans SJ. Acute phase reaction and acute phase proteins. J Zhejiang Univ Sci B. 2005; 6: 1045-56.
37. Landskron G, De la Fuente M, Thuwajit P, Thuwajit C, Hermoso MA. Chronic inflammation and cytokines in the tumor microenvironment. Journal of immunology research. 2014; 2014: 149185.
38. Rosen SD. Ligands for L-selectin: homing, inflammation, and beyond. Annual review of immunology. 2004; 22: 129-56.
39. Arbones ML, Ord DC, Ley K, Ratech H, Maynard-Curry C, Otten G, et al. Lymphocyte homing and leukocyte rolling and migration are impaired in L-selectin-deficient mice. Immunity. 1994; 1: 247-60.
40. Libert C, Hochepied T, Berger FG, Baumann H, Fiers W, Brouckaert P. High-level constitutive expression of alpha 1-acid glycoprotein and lack of protection against tumor necrosis factor-induced lethal shock in transgenic mice. Transgenic research. 1998; 7: 429-35.
41. Ngure RM, Eckersall PD, Jennings FW, Burke JM, Stear MJ, Kennedy PG, et al. Major acute phase response of haptoglobin and serum amyloid-P following experimental infection of mice with Trypanosoma brucei brucei. Parasitology International. 1997; 46: 247-54.
42. Mortensen RF, Beisel K, Zeleznik NJ, Le PT. Acute-phase reactants of mice. II. Strain dependence of serum amyloid P-component (SAP) levels and response to inflammation. J Immunol. 1983; 130: 885-9.
43. Baniyash M, Sade-Feldman M, Kanterman J. Chronic inflammation and cancer: suppressing the suppressors. Cancer Immunol Immunother. 2014; 63: 11-20.
44. Curiel TJ. Tregs and rethinking cancer immunotherapy. The Journal of clinical investigation. 2007; 117: 1167-74.
45. Martin-Orozco N, Li Y, Wang Y, Liu S, Hwu P, Liu YJ, et al. Melanoma cells express ICOS ligand to promote the activation and expansion of T-regulatory cells. Cancer Res. 2010; 70: 9581-90.
46. Ito T, Yang M, Wang YH, Lande R, Gregorio J, Perng OA, et al. Plasmacytoid dendritic cells prime IL-10-producing T regulatory cells by inducible costimulator ligand. The Journal of experimental medicine. 2007; 204: 105-15.
47. Faget J, Bendriss-Vermare N, Gobert M, Durand I, Olive D, Biota C, et al. ICOS-ligand expression on plasmacytoid dendritic cells supports breast cancer progression by promoting the accumulation of immunosuppressive CD4+ T cells. Cancer Res. 2012; 72: 6130-41.
48. Aspord C, Leccia MT, Charles J, Plumas J. Plasmacytoid dendritic cells support melanoma progression by promoting Th2 and regulatory immunity through OX40L and ICOSL. Cancer immunology research. 2013; 1: 402-15.
49. Kadkhoda K, Wang S, Joyee AG, Fan Y, Yang J, Yang X. Th1 cytokine responses fail to effectively control Chlamydia lung infection in ICOS ligand knockout mice. J Immunol. 2010; 184: 3780-8.
50. Manches O, Lui G, Chaperot L, Gressin R, Molens JP, Jacob MC, et al. In vitro mechanisms of action of rituximab on primary non-Hodgkin lymphomas. Blood. 2003; 101: 949-54.
51. Weiner LM, Surana R, Wang S. Monoclonal antibodies: versatile platforms for cancer immunotherapy. Nat Rev Immunol. 2010; 10: 317-27.
52. Nakagawa T, Roth W, Wong P, Nelson A, Farr A, Deussing J, et al. Cathepsin L: critical role in Ii degradation and CD4 T cell selection in the thymus. Science. 1998; 280: 450-3.
53. Yu DM, Slaitini L, Gysbers V, Riekhoff AG, Kahne T, Knott HM, et al. Soluble CD26 / dipeptidyl peptidase IV enhances human lymphocyte proliferation in vitro independent of dipeptidyl peptidase enzyme activity and adenosine deaminase binding. Scand J Immunol. 2011; 73: 102-11.
54. De Meester I, Korom S, Van Damme J, Scharpe S. CD26, let it cut or cut it down. Immunol Today. 1999; 20: 367-75.
55. Hatano R, Ohnuma K, Yamamoto J, Dang NH, Morimoto C. CD26-mediated co-stimulation in human CD8(+) T cells provokes effector function via pro-inflammatory cytokine production. Immunology. 2013; 138: 165-72.
56. Krakauer M, Sorensen PS, Sellebjerg F. CD4(+) memory T cells with high CD26 surface expression are enriched for Th1 markers and correlate with clinical severity of multiple sclerosis. J Neuroimmunol. 2006; 181: 157-64.
57. Kalinski P, Hilkens CM, Snijders A, Snijdewint FG, Kapsenberg ML. IL-12-deficient dendritic cells, generated in the presence of prostaglandin E2, promote type 2 cytokine production in maturing human naive T helper cells. J Immunol. 1997; 159: 28-35.
58. Schoenborn JR, Wilson CB. Regulation of interferon-gamma during innate and adaptive immune responses. Advances in immunology. 2007; 96: 41-101.

59. Pulukuri SM, Gorantla B, Knost JA, Rao JS. Frequent loss of cystatin E/M expression implicated in the progression of prostate cancer. Oncogene. 2009; 28: 2829-38.

60. Tan GJ, Peng ZK, Lu JP, Tang FQ. Cathepsins mediate tumor metastasis. World J Biol Chem. 2013; 4: 91-101.

61. Qiu J, Ai L, Ramachandran C, Yao B, Gopalakrishnan S, Fields CR, et al. Invasion suppressor cystatin E/M (CST6): high-level cell type-specific expression in normal brain and epigenetic silencing in gliomas. Lab Invest. 2008; 88: 910-25.

62. Jin L, Zhang Y, Li H, Yao L, Fu D, Yao X, et al. Differential secretome analysis reveals CST6 as a suppressor of breast cancer bone metastasis. Cell Res. 2012; 22: 1356-73.

63. Kloten V, Becker B, Winner K, Schrauder MG, Fasching PA, Anzeneder T, et al. Promoter hypermethylation of the tumor-suppressor genes ITIH5, DKK3, and RASSF1A as novel biomarkers for blood-based breast cancer screening. Breast Cancer Res. 2013; 15: R4.

64. Ueno T, Elmberger G, Weaver TE, Toi M, Linder S. The aspartic protease napsin A suppresses tumor growth independent of its catalytic activity. Lab Invest. 2008; 88: 256-63.

65. Chen Y, Azman SN, Kerishnan JP, Zain RB, Chen YN, Wong YL, et al. Identification of host-immune response protein candidates in the sera of human oral squamous cell carcinoma patients. PLoS One. 2014; 9: e109012.

66. Li C, Zolotarevsky E, Thompson I, Anderson MA, Simeone DM, Casper JM, et al. A multiplexed bead assay for profiling glycosylation patterns on serum protein biomarkers of pancreatic cancer. Electrophoresis. 2011; 32: 2028-35.

67. Tian M, Cui YZ, Song GH, Zong MJ, Zhou XY, Chen Y, et al. Proteomic analysis identifies MMP-9, DJ-1 and A1BG as overexpressed proteins in pancreatic juice from pancreatic ductal adenocarcinoma patients. BMC Cancer. 2008; 8: 241.

68. Kreunin P, Zhao J, Rosser C, Urquidi V, Lubman DM, Goodison S. Bladder cancer associated glycoprotein signatures revealed by urinary proteomic profiling. J Proteome Res. 2007; 6: 2631-9.

69. Holm AT, Wulf-Johansson H, Hvidsten S, Jorgensen PT, Schlosser A, Pilecki B, et al. Characterization of spontaneous airspace enlargement in mice lacking microfibrillar-associated protein 4. Am J Physiol Lung Cell Mol Physiol. 2015: ajplung 00351.2014.

70. Johansson SL, Roberts NB, Schlosser A, Andersen CB, Carlsen J, Wulf-Johansson H, et al. Microfibrillar-associated protein 4: a potential biomarker of chronic obstructive pulmonary disease. Respir Med. 2014; 108: 1336-44.

71. Gabay C, Kushner I. Acute-phase proteins and other systemic responses to inflammation. The New England journal of medicine. 1999; 340: 448-54.

72. Gabrilovich DI, Nagaraj S. Myeloid-derived suppressor cells as regulators of the immune system. Nat Rev Immunol. 2009; 9: 162-74.

73. Trinchieri G. Cancer Immunity: Lessons From Infectious Diseases. The Journal of infectious diseases. 2015; 212 Suppl 1: S67-73.

74. Zhang S, Danchuk SD, Bonvillain RW, Xu B, Scruggs BA, Strong AL, et al. Interleukin 6 Mediates the Therapeutic Effects of Adipose-Derived Stromal/Stem Cells in Lipopolysaccharide-Induced Acute Lung Injury. Stem Cells. 2014; 32: 1616-28.

75. Chen Q, Fisher DT, Kucinska SA, Wang WC, Evans SS. Dynamic control of lymphocyte trafficking by fever-range thermal stress. Cancer Immunol Immunother. 2006; 55: 299-311.

76. Evans SS, Wang WC, Bain MD, Burd R, Ostberg JR, Repasky EA. Fever-range hyperthermia dynamically regulates lymphocyte delivery to high endothelial venules. Blood. 2001; 97: 2727-33.

77. Wang WC, Goldman LM, Schleider DM, Appenheimer MM, Subjeck JR, Repasky EA, et al. Fever-range hyperthermia enhances L-selectin-dependent adhesion of lymphocytes to vascular endothelium. J Immunol. 1998; 160: 961-9.

78. Fisher DT, Chen Q, Skitzki JJ, Muhitch JB, Zhou L, Appenheimer MM, et al. IL-6 trans-signaling licenses mouse and human tumor microvascular gateways for trafficking of cytotoxic T cells. The Journal of clinical investigation. 2011; 121: 3846-59.

79. Ljungberg B, Grankvist K, Rasmuson T. Serum interleukin-6 in relation to acute-phase reactants and survival in patients with renal cell carcinoma. Eur J Cancer. 1997; 33: 1794-8.

80. Martin F, Santolaria F, Batista N, Milena A, Gonzalez-Reimers E, Brito MJ, et al. Cytokine levels (IL-6 and IFN-gamma), acute phase response and nutritional status as prognostic factors in lung cancer. Cytokine. 1999; 11: 80-6.

81. Lippitz BE. Cytokine patterns in patients with cancer: a systematic review. The Lancet Oncology. 2013; 14: e218-28.

82. Mold C, Baca R, Du Clos TW. Serum amyloid P component and C-reactive protein opsonize apoptotic cells for phagocytosis through Fcgamma receptors. Journal of autoimmunity. 2002; 19: 147-54.

83. Le Friec G, Kemper C. Complement: coming full circle. Arch Immunol Ther Exp (Warsz). 2009; 57: 393-407.

84. Peng Q, Li K, Anderson K, Farrar CA, Lu B, Smith RA, et al. Local production and activation of complement up-regulates the allostimulatory function of dendritic cells through C3a-C3aR interaction. Blood. 2008; 111: 2452-61.

85. Strainic MG, Liu J, Huang D, An F, Lalli PN, Muqim N, et al. Locally produced complement fragments C5a and C3a provide both costimulatory and survival signals to naive CD4+ T cells. Immunity. 2008; 28: 425-35.

86. Papp K, Vegh P, Prechl J, Kerekes K, Kovacs J, Csikos G, et al. B lymphocytes and macrophages release cell membrane deposited C3-fragments on exosomes with T cell response-enhancing capacity. Mol Immunol. 2008; 45: 2343-51.

87. van Montfoort N, de Jong JM, Schuurhuis DH, van der Voort EI, Camps MG, Huizinga TW, et al. A novel role of complement factor C1q in augmenting the presentation of antigen captured in immune complexes to CD8+ T lymphocytes. J Immunol. 2007; 178: 7581-6.

88. Jiang K, Chen Y, Xu CS, Jarvis JN. T cell activation by soluble C1q-bearing immune complexes: implications for the pathogenesis of rheumatoid arthritis. Clinical and experimental immunology. 2003; 131: 61-7.

89. Longhi MP, Wright K, Lauder SN, Nowell MA, Jones GW, Godkin AJ, et al. Interleukin-6 is crucial for recall of influenza-specific memory CD4 T cells. PLoS Pathog. 2008; 4: e1000006.

90. Sallusto F, Geginat J, Lanzavecchia A. Central memory and effector memory T cell subsets: function, generation, and maintenance. Annual review of immunology. 2004; 22: 745-63.

91. Newson J, Stables M, Karra E, Arce-Vargas F, Quezada S, Motwani M, et al. Resolution of acute inflammation bridges the gap between innate and adaptive immunity. Blood. 2014: blood-2014-03-562710.

Author Biography

Dr. Lisa X. Xu received her Ph.D. degree in 1991 at the University of Illinois at Urbana-Champaign. In 1997, she became a tenured associate professor in Mechanical Engineering of Purdue University. Now she is a Chair professor in the School of Biomedical Engineering at Shanghai Jiao Tong University in China. Her research focuses on bio-thermal physics, and cancer diagnosis and thermal therapy. She has coauthored over 150 publications and written 4 book chapters. Dr. Xu received the "Chang Jiang Scholar" Distinguished Professorship Award from Chinese Ministry of Education in 2003, the "Outstanding Youth Award" by Chinese Natural Science Foundation (CNSF) in 2007, and the 2nd Natural Science Award from Chinese Ministry of Education in 2010. She is an elected fellow of ASME, AIBME, and a senior member of IEEE. She also serves as the President of Shanghai Society of Biomedical Engineering since 2010.

Dr. Wei Yan received his B. S. at Nanjing University (China) in 1988 and Ph.D. degree in 1999 on Biomolecular Chemistry at the University of Wisconsin-Madison under Dr. Elizabeth Craig. After a post-doctoral training at University of Washington with Dr. Michael Katze, he joined laboratory of Dr. Ruedi Aebersold at Institute for Systems Biology (ISB) to practice proteomics using mass spectrometry in 2002 and later practiced systems

biology as well with Drs. Leroy Hood and Jeff Ranish, as a senior research scientist. In 2013 he joined the faculty of Shanghai Center for Systems Biomedicine at Shanghai Jiao Tong University in China. His research interest includes technology development on targeted quantitative proteomics and translational applications of various proteomics technologies in discovering and validating disease-specific protein biomarkers used for cancer diagnosis and therapy.

Prof. Robert L. Moritz has a Bachelor's degree in Biochemistry with first-class Honors, and his Ph.D., from the University of Melbourne. He joined the Institute Systems Biology (ISB, WA, USA) faculty in 2008 as Director of Proteomics Research after a 25 year career at the Ludwig Institute for Cancer Research, Melbourne, Australia. Prof. Moritz has authored more than 220 peer-reviewed papers and holds multiple patents in technology development and therapeutic protein identification. His group at the ISB performs proteomics research into diseases involving the lung, colon, prostate and brain with a focus on cancer, infectious disease and wellness studies.

Dr. Ping Liu received her B.S. and M.S. degrees at Sichuan Agricultural University (China) in 1994 and 1997, and the Ph.D. degree at Shanghai Jiao Tong University (China) on life sciences and biotechnology in 2005. From 1999 to 2008, she joined the School of Agriculture and the School of Life Sciences and Biotechnology at Shanghai Jiao Tong University as an assistant professor. In 2009, she became the associate professor in the team of Dr. Lisa X. Xu at the School of Biomedical Engineering and Med-X Research Institute. Her research interests include cancer thermal therapy, and the mechanism of biological and immunologic effects induced by cryo-thermal therapy.

Ting Xue is currently a Ph.D. student under the supervision of Dr. Lisa X. Xu. She has a five-year experience in shotgun and target proteomics. Her research focuses on the understanding of breast cancer metastasis based on membrane proteome and the immune response induced by breast cancer therapy.